

**Robotic 3D printing of concrete printed building
components: a design-to-fabrication algorithmic framework
for efficient housing construction in Saudi Arabia**

1st Mohammad Alabbasi ^a, 2nd Asterios Agkathidis ^b, 3rd Hanmei Chen ^c

^a 1st Author Affiliation, City, Country, e-mail address

^b 2nd Author Affiliation, City, Country, e-mail address

^c 3rd Author Affiliation, City, Country, e-mail address

Highlights

Abstract

This article examines the creation of a design and fabrication framework aiming to increase the efficiency of the construction of reinforced concrete building components in Saudi Arabia through 3D concrete printing. To illustrate this, the research presents a design-to-fabrication algorithmic framework to mass-customise a typical Saudi house utilising parametric modelling, topology optimization (TO), finite element analysis (FEA), and robotic 3D printing techniques. The framework was validated by manufacturing four 3D printed reinforced concrete columns and testing their structural performance under the Saudi Building Code. The findings demonstrate the benefits and drawbacks of the proposed design-to-fabrication framework compared to current Saudi conventional construction approaches. The design specification process is generated by numerical values of design constraints, objectives, and condition boundaries, which make it possible to develop a novel algorithmic AM framework using high computational and data bandwidths. Furthermore, adopting robotic-based printers to 3D-print structural building components would increase construction production efficiency and address KSA citizens' customisation issues, which centralised precast manufacturing has failed to solve.

Keywords

Add about 5 keywords or phrases separated by semicolons for use in indexing this paper; these may also be used to identify appropriate reviewers. For the Keywords heading, use the Normal style and bold it.

1. Introduction

The construction industry is a practically value-creating enterprise in the sense of facility or asset creation, owing to its broad breadth and significant support to all other industries. Due to increased urbanisation in many nations, the construction sector is expected to account for 13% of global GDP [1]. In Saudi Arabia, the overall GDP of the construction industry is 2.62 trillion Saudi Riyals in 2020 [2]. Saudi Arabia's construction industry is the second largest after the oil industry [3]. Thus, the construction industry's enormous scale necessitates consideration of its efficiency and environmental impact. The worldwide economy and the global

population stand to benefit significantly from even small increases in the construction industry's operational effectiveness. Moreover, digital technology is a game-changer in the construction sector, enabling essential transformation. Various elements of human existence have been revolutionised by digitalisation throughout the last three decades, and enterprises have been revamped. In terms of digitalisation and productivity advances, the construction sector lags behind most industrial enterprises [4]. Unlike many other industries, the construction industry has yet to be significantly disrupted by digital technology [5].

In-situ reinforced concrete fabrication is now the most common house construction technique in Saudi Arabia. However, this approach is inefficient due to high labour demand, poor building quality, and time requirements [6]. Thus, home residents in Saudi Arabia prefer a custom-built home versus a conventional residence [7,8]. This study aims to provide a novel design-to-fabrication framework that integrates 3D concrete printing with robotic fabrication. The proposed design-to-fabrication framework will apply the Saudi Concrete Building Structures (SBC 304) standards and specifications for the manufacturing of 3D printed reinforced concrete components.

The research objectives are the following: to eliminate waste of formwork materials, reduce labour intensity, and shorten construction time through the use of robotic technology. The research will examine the employment of robotics in construction to improve construction efficiency and speed up construction, hence improving construction productivity. As a result, the following research questions should be addressed:

- 1. How can we develop a framework for the design and 3D printing of a reinforced concrete frame structure of a typical Saudi house?*
- 2. How can the developed framework contribute to the faster and more efficient construction of structural building components and enable mass customisation?*
- 3. How will the framework be implemented and validated with regard to the Saudi Arabian Building Code (SBC 304)?*

Three phases will address the aforementioned questions: a) parametric design, classification, and topology optimisation of a typical Saudi villa; b) prototyping of a 3D printed reinforced concrete column; and c) mechanical axial load testing the column's performance and functionality.

2. Background and Literature review

Additive manufacturing of concrete

Concrete additive manufacturing (AM) technologies, often known as cement-based 3D printing, have advanced fast over the last decade, demonstrating their ability to rationalise the construction sector. Concrete AM can create high-precision construction components at a low cost and in a short time [9]. As a result, the quantity of labour required can be minimised. To manufacture concrete layers, most AM solutions in the construction sector use an extrusion-based material approach based on sliced CAD geometry [10]. This method allows for more freedom in the construction of complicated geometries without the necessity of conventional plywood concrete moulds [11]. AM of concrete can be implemented in-situ or as a prefabricated component. The manufacture of building walls is a frequent application of in-situ 3D printing concrete in-situ, as seen in the BOD building by COBOD in Denmark, Studio 2030 by CyBe in Saudi Arabia, and the Dubai municipality building by ApisCore in the UAE [12]. These precedents are only examples of what is possible. However, there is a clear disconnect between building regulations and AM technology, necessitating a strategy to bridge the gap.

The use of AM in building construction appears to have advantages over traditional construction methods. The decrease in construction time and cost is one of these benefits. Other notable benefits include an improvement in construction workers' health and safety requirements, and the formal latitude granted to architects, allowing them to implement complicated designs [13]. However, one of AM's drawbacks in construction is the lack of a full design to fabrication framework that allows for a direct relationship between the design output and the fabrication process [14]. Another significant limitation identified by Buswell et al. 2018 [10] is the geometrical agreement with material properties. The geometrical printability and standardisation of 3D printing concrete components are high-priority concerns that need to be addressed by codes and regulations [15], as existing building regulation in Saudi Arabia is not directly relevant to 3DCP, which require testing of concrete properties [16].

Topology optimisation for additive manufacturing

Topology optimisation (TO) is a mathematical approach of geometrical connection that optimises the structural system's performance based on a particular load and boundary condition [17]. The use of TO in

construction is not a new concept. TO has been utilised to boost structural efficiency by increasing structural rigidity while reducing material usage [18].

"Illa de Blanes," a multi-space project in Spain, is one of the earliest examples of TO in architecture. The research used a digital evolutionary structural optimisation approach (ESO). Another structure that used the TO application is the Akutagawa office building in Takatsuki, Japan, designed by F-Tai architects alongside structural engineer Hiroshi Ohmori in 2005. The extended evolutionary structural optimisation (ESO) approach was used as the major optimisation procedure in this four-story structure. The ESO approach was used to determine the form of the building's walls. Its architectural and structural designs are successful in blending with the building's exterior. As part of the optimisation procedure, other structural elements such as live, dead, and seismic loads were taken into account. The TO's outputs were confirmed in an elastoplastic numerical model based on structural deflections and cracking patterns [19]. Reinforced concrete was used to construct the building's structural frame. It necessitated the deployment of a complicated formwork, which is one of the drawbacks of employing traditional building methods to incorporate TO in architecture [20].

Furthermore, Ohmori and Sasaki's Qatar National Convention Centre (QNCC) in Doha is another project that was completed using a TO approach in 2011. [19]. The project created the XESO (extend ESO) approach, which was used on the huge roofs of the structures (36m wide x 150m long). The project's engineers, Buro Happold consulting, introduced characteristics such as constructability and geometrical rationality into the design process. As a result, the optimised shape was reduced, and a steel frame structure was recommended to expedite the building process and save costs [20].

In order to develop an efficient lattice structure, a voxel-based 3D model is frequently employed in topology optimisation. The term voxel refers to a 3D representation of a pixel. The voxel 3D model is a volume representation rather than a set of boundaries. As a result, the material distribution might be more effective. The density of a weak region will be raised, while the density of a strong area will be lowered [21,22].

As a result of the precedence stated here, we have chosen to employ the TO approach, also known as 'the material distribution and boundary variation method', which provides for optimal material distribution to the final object. The Solid Isotropic Material with Penalisation Method (SIMP) will be part of this methodology [23]. It will also be used in conjunction with voxel-based modelling to forecast the best material

distribution/robustness depending on the input data. The material distribution technique, in general terms, is an element-based method that uses optimisation algorithms in conjunction with the finite element method to find a solution for a structural element, with design parameters serving as components or attributes of the components [21]. When it comes to determining the optimal structure, this technique has been proven to be beneficial in topology optimisation applications. Furthermore, in our experiment, additive manufacturing technology will be employed as a fabrication technique. Our goal is to minimise wasteful material consumption, improve safety, quality, and productivity on the building site by integrating AM of concrete with TO.

Design for additive manufacturing (DFAM)

Digital design for AM (DFAM) provides knowledgeable designers with a substantial opportunity to design a feasible printable object while improving performance and efficiency. The design process involves three design stages: a) conceptual design, b) embodiment, and c) detail design. The choosing of the optimum design solutions is based on the design stages' results based on the given parameters. In the design consideration stage, a set of files of data is created to describe the exterior part of the envelope geometry of AM that is defined formally as the desired CAD for the geometry. This data based on geometry volumetrics is consistent with the designs that come later, for instance, slice geometry data, and have reasonable computational and storage efficiency. There are different formats of geometry to select from, and each one has its own resolution, compatibility and characteristics representing each size [17]. Although it is not absolutely essential, the specification that is formal and supports the structures of AM is universally conducted by aligning with the geometry phase of the volumetric, especially for the DFAM that has digitally enhanced possibilities that skip the formal descriptions. The support creation of structures is still an ongoing area of research in the DFAM field that allows for considerable economic benefits by using optimal digital design strategies [17].

Laverne et al. (2014) indicated a significant shortage of DFAM tools and approaches aimed at the early stages of the design process [24]. This shortcoming is most likely due to a misalignment of market pull and research push. DFAM tools account for a toolpath's impact on mechanical and functional characteristics.

Most AM products have hundreds of distinct slicing levels, each with its own toolpath. For structurally important practical AM applications, DFAM techniques that actively reduce flaws inside these layers are critical. Developing sophisticated DFAM tools is complicated by the lack of established digital toolpath standards.

3. Methodology

The research was conducted utilising a physical–empirical method that originated principally from the development of a design–to–fabrication framework. This entailed using robotic fabrication technology to perform TO and AM on a reinforced concrete component and creating a physical architectural model (Figure 1). Additionally, the study was fundamentally multidisciplinary in nature and was conducted using principles of architectural and structural design, material science, mechanical engineering, and robotics. The proposed methodology depicted in Figure 1 is divided into three distinct steps. The first stage denotes the beginning of the computational framework in a Rhino/Grasshopper environment. The second stage involves developing digital and physical prototypes of reinforced-concrete columns with optimised topology. In the third stage, a mechanical load test was performed to ensure structural function and performance. However, only the load-bearing system was considered in this study, as walls and finishing are not included.

After identifying the primary challenges and reviewing Saudi Arabia's requirements for concrete structures (SBC 304) [25], the proposed design-to-fabrication framework will satisfy the Kingdom's requirements and specifications for the production of 3D-printed reinforced concrete components. As such, the framework is validated by creating a parametric reinforced-concrete frame structure for a typical Saudi house. A column will be optimised and analysed to determine its resilience when subjected to an axial load. As specified in SBC 304, the compressive strength of the concrete should not be less than 20 MPa [25]; hence, C40 self-consolidating concrete was developed during the prototyping phase.

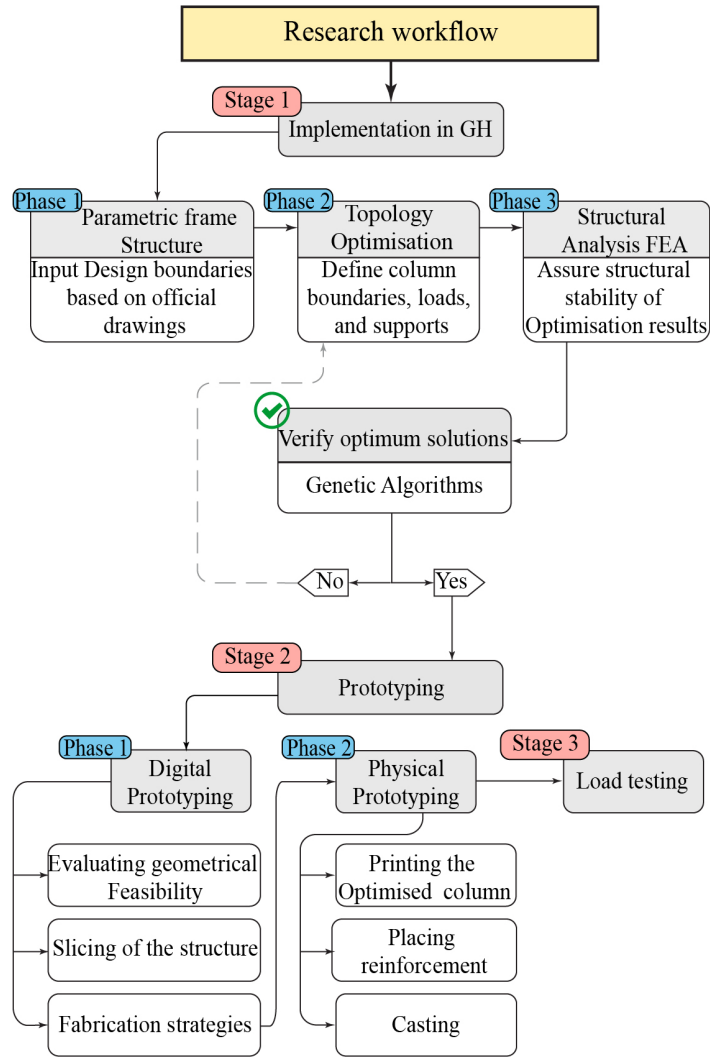


Figure 1: Design-to-Fabrication Framework

3.1. Stage 1: Design and topology optimisation for AM of concrete

The first stage consists of three phases: 1) the development of an algorithmic design-to-fabrication framework; 2) the TO of a reinforced concrete column, and 3) structural analysis of the TO results (Figure 2). The next subsections discuss how the first stage was implemented, with a particular emphasis on the TO of a reinforced-concrete column:

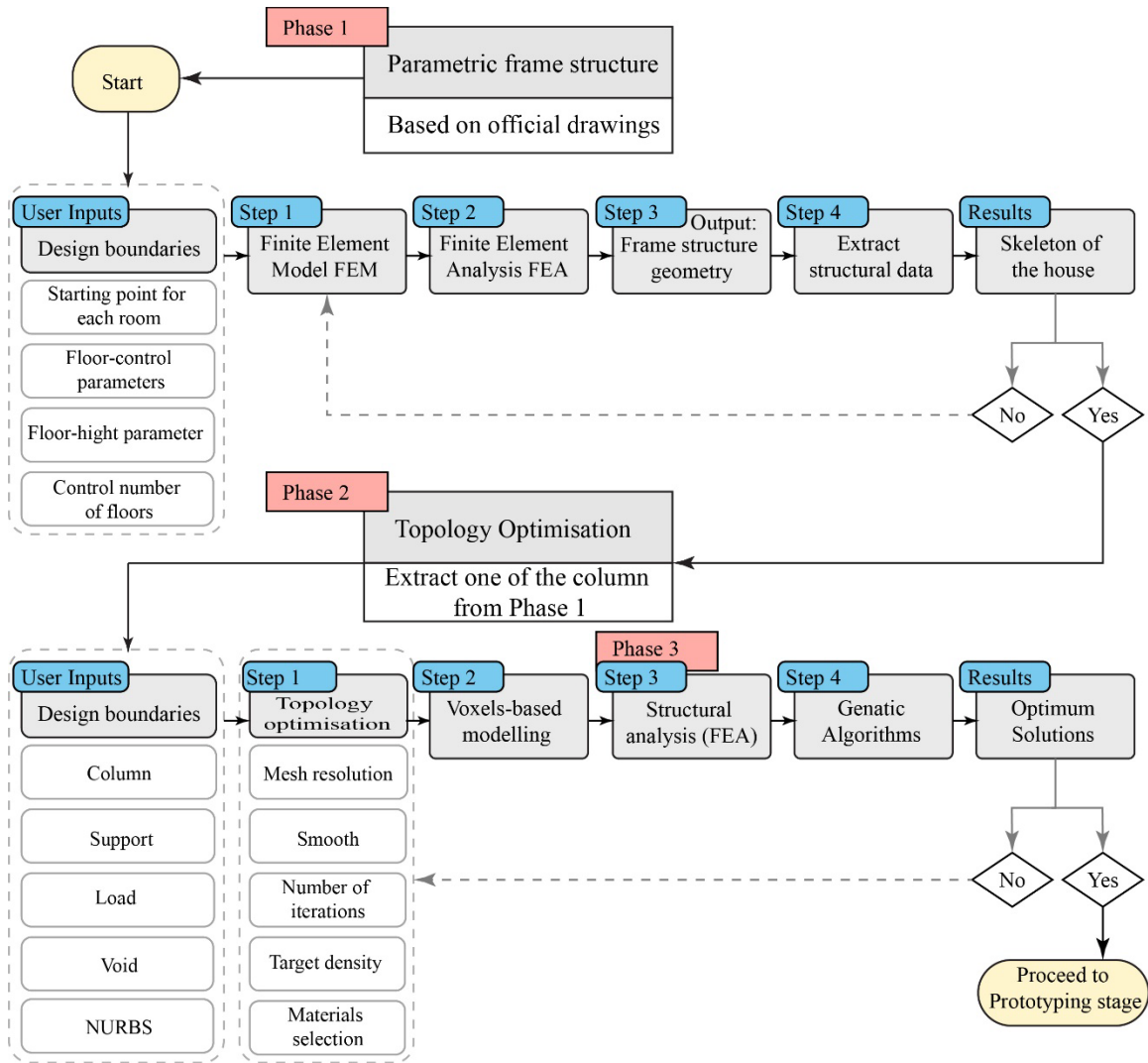


Figure 2. Design and optimisation workflow

3.1.1. Phase 1: Parametric reinforced-concrete frame structure of a typical Saudi villa

The FE parametric model was developed using a floor plan scheme for a typical single-family 'villa', which was obtained by the Saudi Ministry of Housing. The parametrisation of the frame structure of the authentic villa in Rhino/Grasshopper was implemented using the structural modelling tool Karamba (Figure 3). The results of the Karamba model created a finite element model (FEM) that accurately reflected the concrete frame structure of the house (Figure 4). After developing the parametric frame structure from an official

drawing, the findings were compared to the official drawing obtained from the Saudi Ministry of Housing to guarantee that the simulated model was identical to the original house layout. Following that, structural data for structural elements were extracted (e.g. columns, beams and slabs).

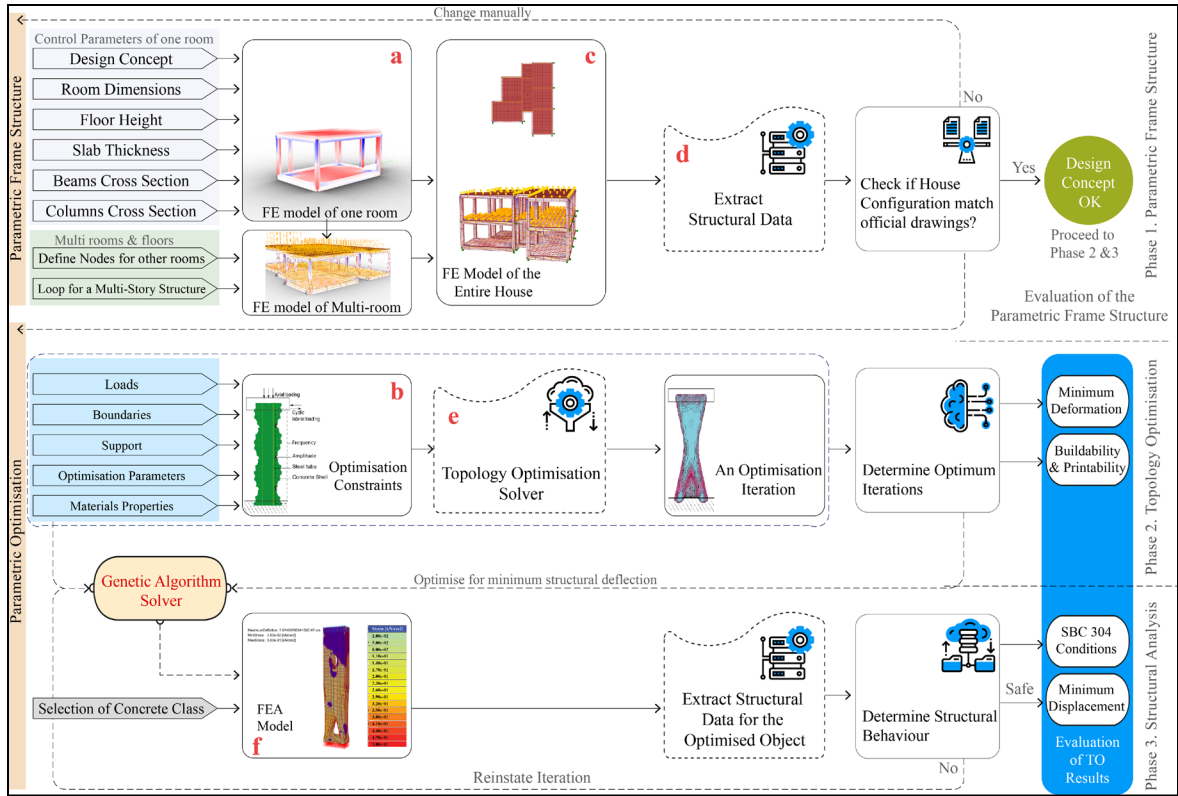


Figure 3: Conceptual illustration for Grasshopper algorithm including floorplan control parameters

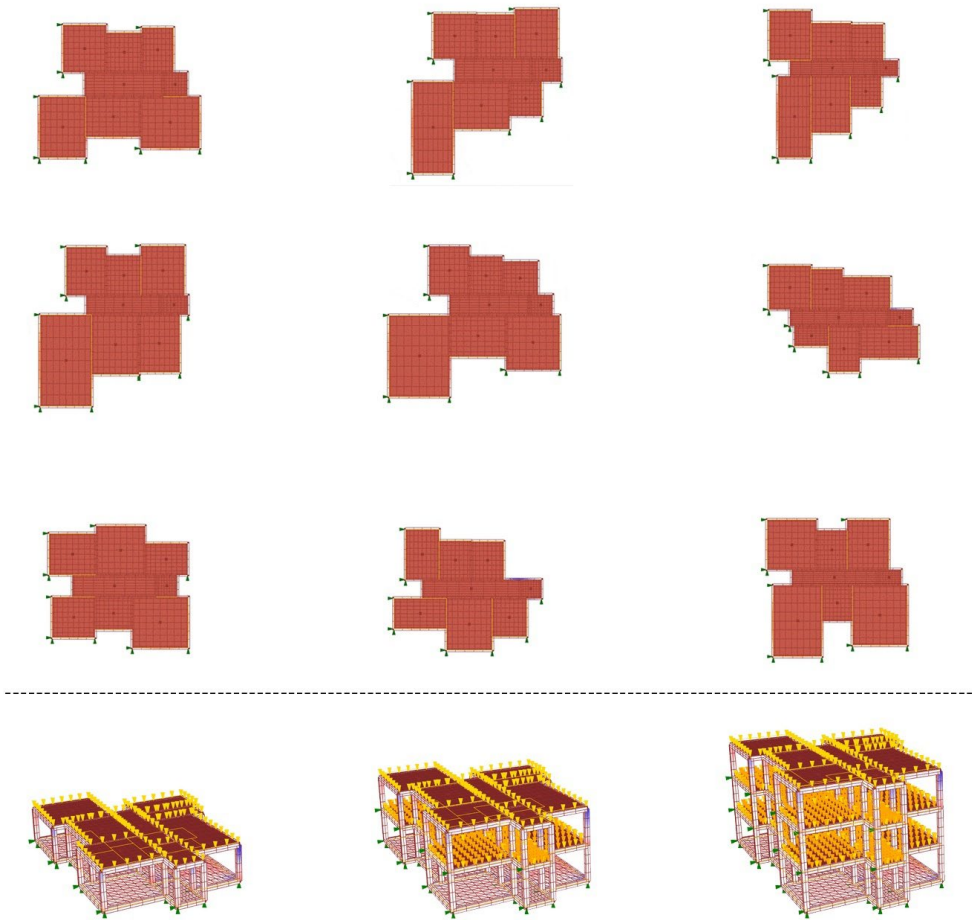


Figure 4: Finite element parametric model generated using Grasshopper script

Although the entire process was validated by testing one of the reinforced columns and comparing its efficiency (material waste, labour demand, and construction duration) to a conventionally designed and fabricated column, the same process (i.e. beams and slabs) can be applied to other structural elements (i.e. beams and slabs) using the developed GH script as shown in Figure 5. As a result, the slabs can be separated and printed as small segments that can be assembled on the construction site in the same manner that hollow-core slabs assembled in-situ. The divided structural components can be printed utilising a transportable container factory for in-situ construction.

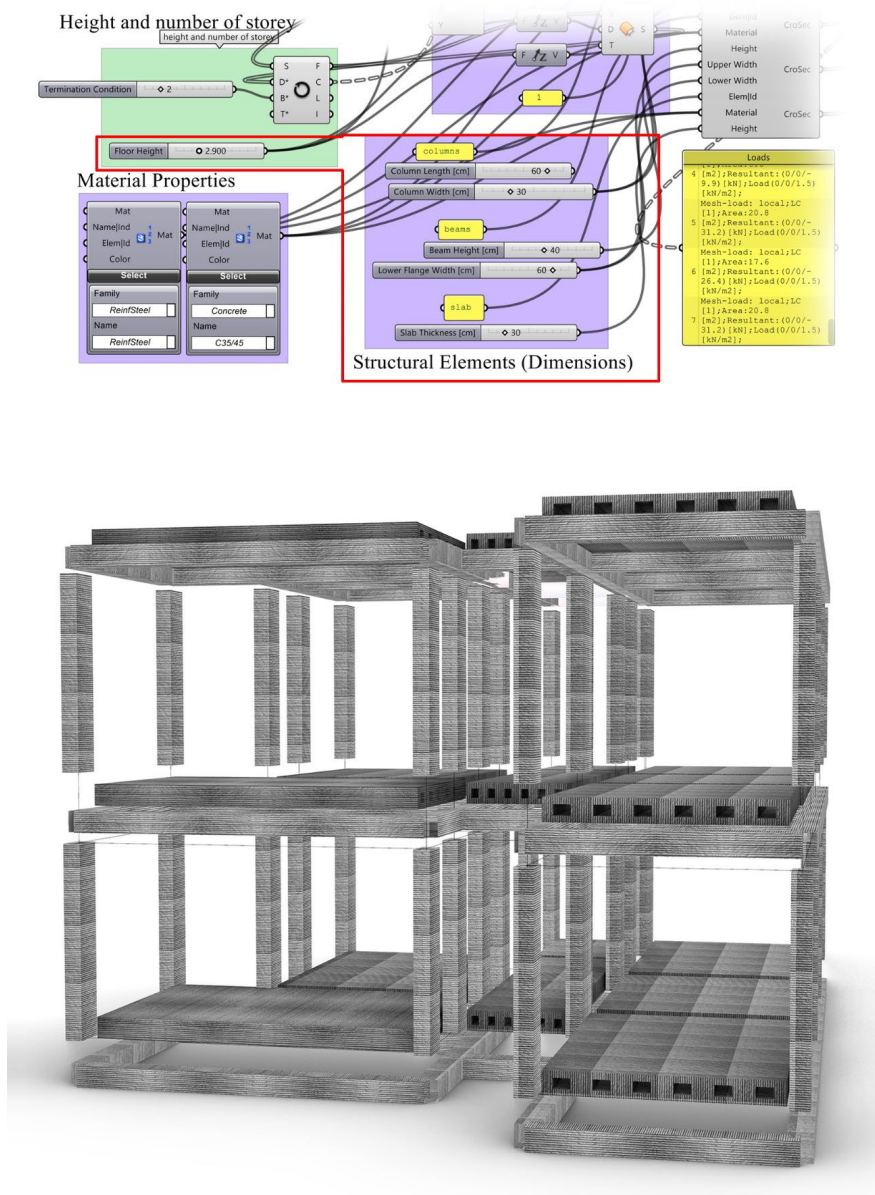


Figure 5: Dividing structural elements and preparation for the fabrication process

3.1.2. Phase 2: Topology optimisation of a reinforced-concrete column

The TO of the column was carried out in three steps to achieve minimum structural deflection: 1) setting the column boundaries, 2) topology optimisation conditions, and 3) verification of the optimisation script (Figure 6). The column boundaries were determined using a surface box with dimensions of $0.3 \text{ m} \times 0.6 \text{ m} \times 2.90 \text{ m}$ (width \times length \times height).

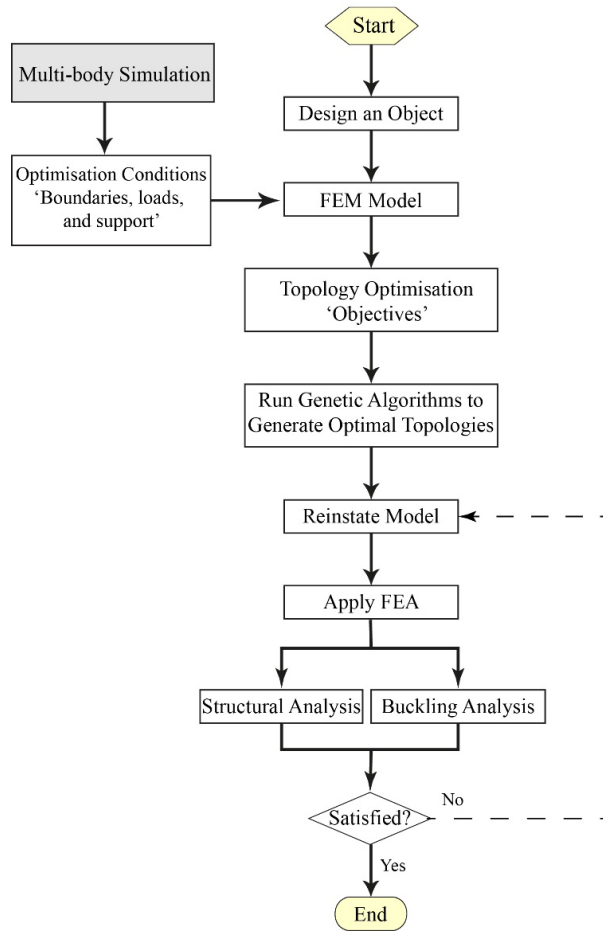


Figure 6: Optimisation workflow implemented in the research using Millipede

The model was fed into a topology optimisation processor (Millipede plug-in). The optimisation technique is used to distribute materials with the least amount of tension in order to precisely delete materials. The applied load on the column was estimated as part of the house's FEM, which was discussed in Stage 1. Thus, the computed load was multiplied by 1000 to convert from kN to N because Karamba's units were different from those of Millipede's inputs. Moreover, a voxelisation-based method was used to take advantage of the Monolith Grasshopper plug-in. The optimisation parameters (i.e. iterations number, smooth, and density) were then fed into the evolutionary solver Galapagos, which is a heuristic solver that compares approximate solutions [26]. Galapagos took into account the number of optimisation iterations, target density, and material density as input parameters. The Galapagos solver compared several outputs based on the input variables, with the goal of maximising structural stiffness and minimising

structural deflection, as well as producing optimal solutions. To comply with SBC304 requirements the steel reinforcement was pre-located in the conceptual embedment stage, as shown in Figure 7.

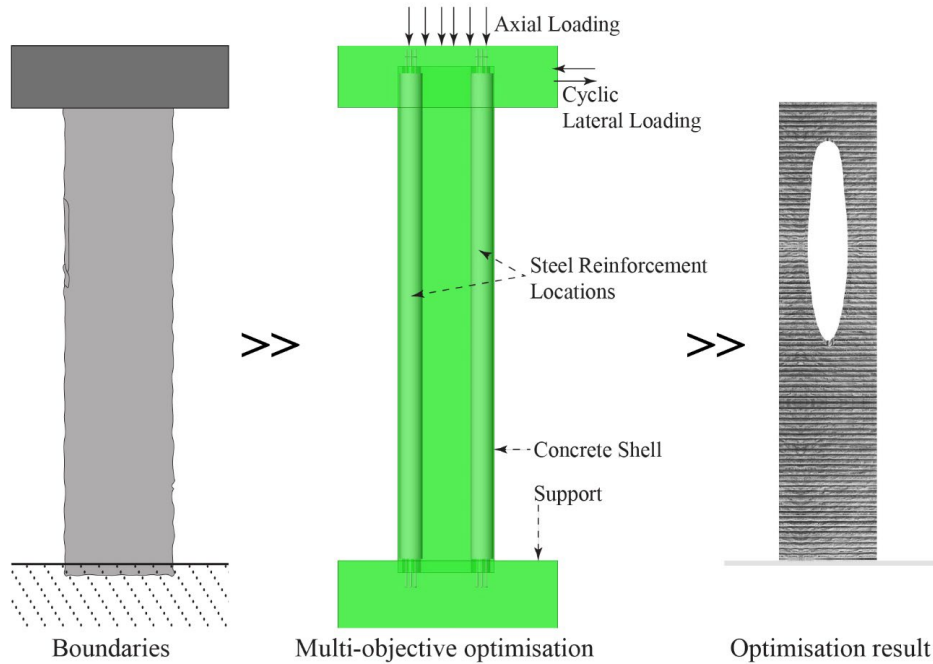


Figure 7: Topology optimisation objectives in the GH script to meet SBC 304 steel reinforcement requirements

3.1.3. Phase 3: Structural analysis

The x-axis mesh resolution was set to 12 as recommended by the software manual, to reduce time and memory used for optimisation, and allow the Millipede plug-in to efficiently voxelise the main boundaries and create the primary FEM. Thus, the Karamba Grasshopper plug-in was used to analyse the performance of the optimised structure after applying the Galapagos plug-in. In this step, the SBC 304 was used to verify the structural analysis [27]. The column was tested in C40 concrete with a 31.2 kN/m^2 vertical load and a fixed base support. The Karamba simulation solver visualised the expected structural stress. The structure's minimum stress was $2.00\text{e-}02 \text{ kN/cm}^2$, and its maximum was $5.00\text{e-}01 \text{ kN/cm}^2$ (Figure 8). The structural analysis was carried out to compare multiple TO iterations in order to find the best geometry that can be 3D printed without supporting material. The FE approach was utilised to find a load scenario that would demonstrate the difference in compression and tensile stress handling.

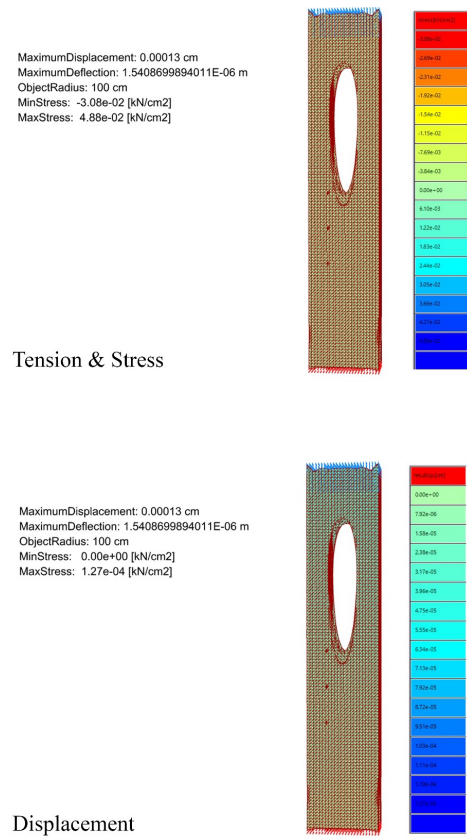


Figure 8. Example of simulation results of the optimised column showing maximum and minimum stress and deflection

3.2. Stage 2: Prototyping

The second stage was to build prototypes to test the general framework (Figure 1). The column's validity had to meet SBC 304 requirements. To do this, the topologically optimised concrete column was digitally and physically prototyped. Consequently, designers can benefit from design-to-fabrication approaches while addressing digital AM design difficulties and challenges. The inherent digital aspect of AM design allows for significant design innovation. These rely on AM's reliability, reproducibility, and efficiency, as well as detailed validation documentation. In addition, physical prototyping was used to experimentally evaluate the computational framework processes using AM-optimised reinforced concrete column prototypes.

3.2.1. Phase 1: Digital prototyping

- Evaluating geometrical feasibility

The optimised column was contoured with a layer height of 10 mm to identify the best printing method and orientation. This was conducted to assess the printability of the printed object and detect buildability challenges, as elastic and plastic collapse are the main failure mechanisms of 3D-printed concrete. Weakness could not emerge only as a result of thixotropic behaviour due to the enormous overhangs at the top of the hole (Figure 9). A 2-component nozzle was considered to 3D print the column, allowing for high tensile capacity while avoiding buildability restrictions.

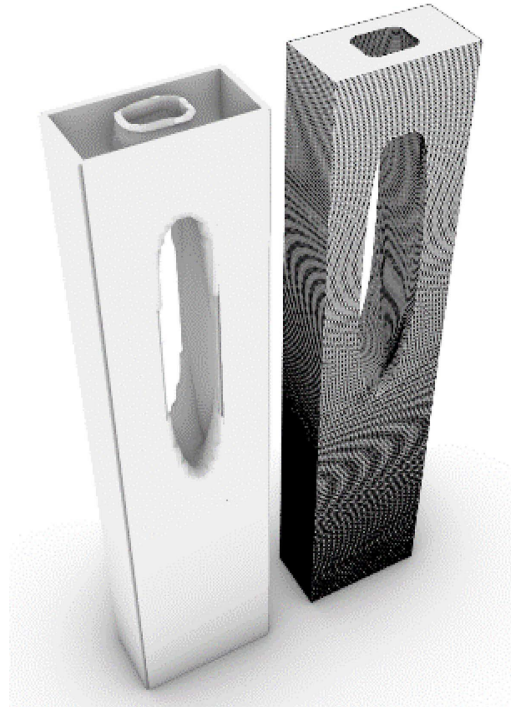


Figure 9. Illustration of a watertight model with overhangs at the centre of the column as a result of topology optimisation



Figure 10. Evaluation of difficult layers

When analysing buildability, the bottom of the hole in the column was unsupported. Therefore, two different strategies can be employed to address the lack of support:

- Adding support material to the column's bottom during printing to sustain the printed layers.
- Printing the column upside-down reduces material waste and production time (Figure 11).

As filling the column with support material would require a significant increase in labour, printing the formwork upside-down was the most reasonable route to take in terms of formwork manufacturing to achieve the research objectives.

Multiple curves could be detected at the same layer height while contouring the object, necessitating start-stop processes (Figure 11). Thus, as the research objective required mitigation in construction duration and labour, it was essential to 3D-print the column in one go. Hence, an optimal printing strategy had to be devised to reduce the number of start-stop processes. Because of the accelerated concrete's rapid setting behaviour and the increased layer-to-layer duration, start-stops were undesirable. It was therefore necessary to devise a method for printing the structure with the fewest possible start-stops while taking into consideration probable collisions. As a result, the method depicted in Figure 11 was developed, using a 450 mm extendable nozzle.

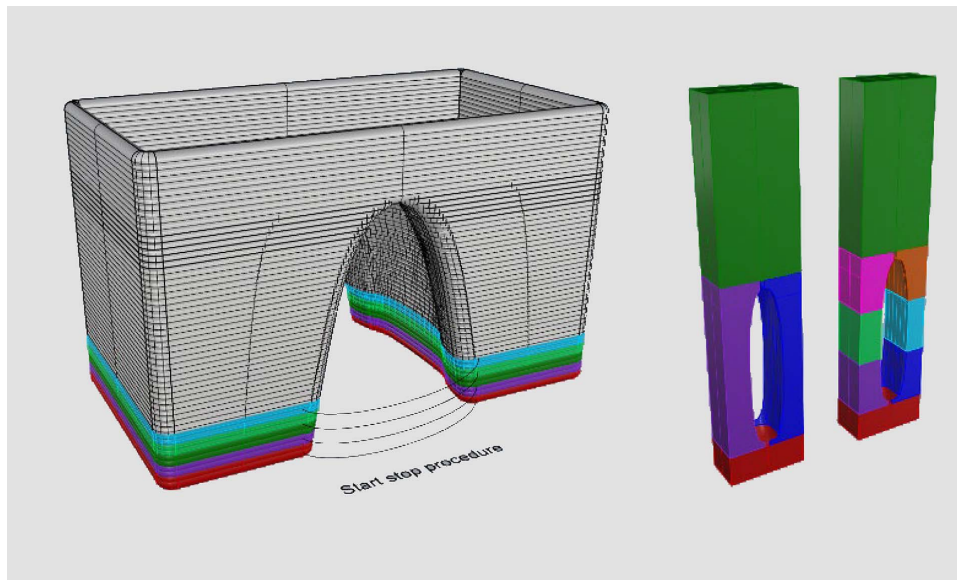


Figure 11: Proposing a start and stop-process for the robotic arm and segmenting the column into fragments

- Slicing of the topologically optimised structure and robotic simulation

The simulation of the fabrication process was part of the computational workflow. This was accomplished by directly connecting the firmware for the offline robot simulation software, RoboDK, to the Grasshopper environment (Figure 12). This enabled viewing the robotic arm's movement and ensuring that all contours were reachable during manufacturing. Moreover, the end-effector could be integrated into the simulation of the robotic arm, allowing for geometrical verification of collisions between previously printed layers and the robotic arm's trajectory. Finally, the simulation provided a glimpse of the structure's gradual construction (Figure 13).

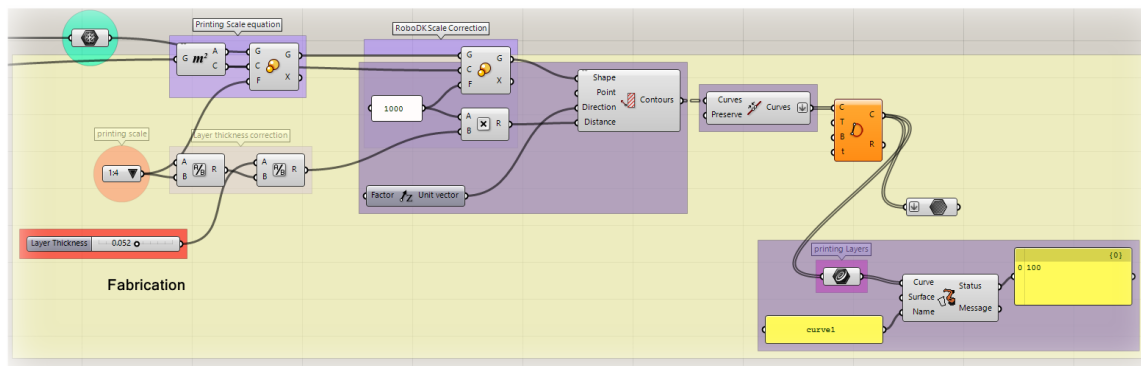


Figure 12: GH script enables the slicing and robotic fabrication of TO results

The model was contoured and scaled using the Grasshopper plug-in, RoboDK, an offline programming firmware suite used for robotic fabrication applications (Figure 13). Its integration with Grasshopper is essential for toolpath generation, as the slicing algorithm can adjust the printing layers' height and the printing speed, according to the material's properties. Eventually, the 3D printing process was simulated again using RoboDK. The layer height was 7 mm, and the printing speed was 160 mm/sec. However, these variables were parameters and could be modified based on material properties, as illustrated in the RoboDK simulation (Figure 13).

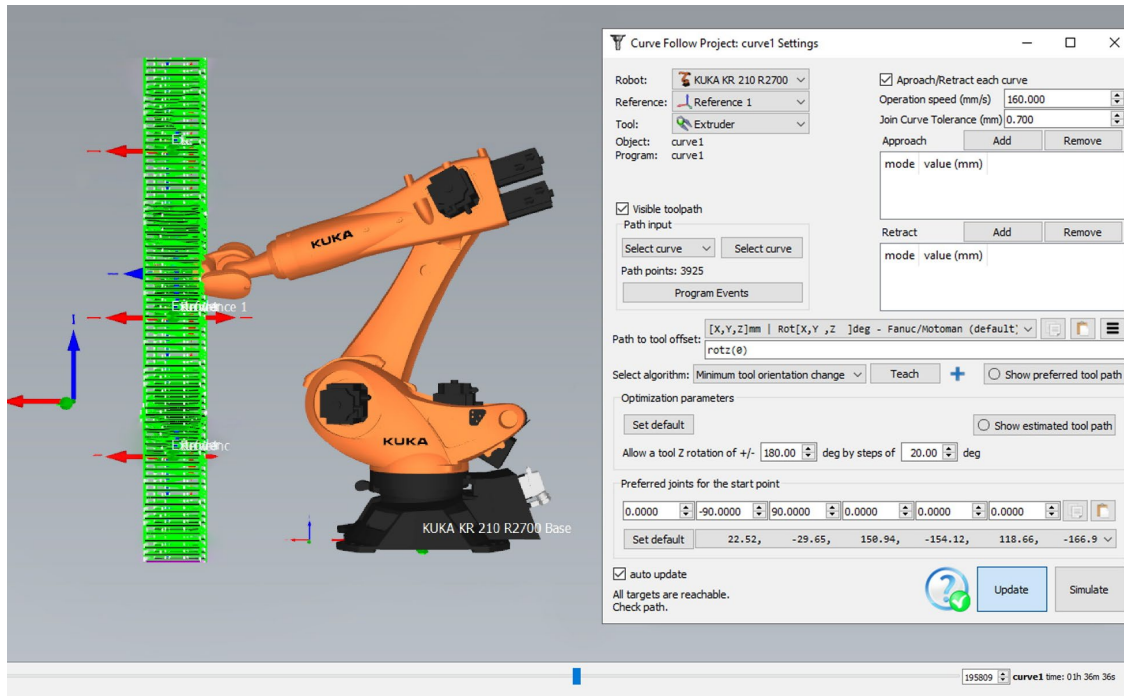


Figure 13: Example of robotic simulation for a scale model using RoboDK

The creation of AM concrete and robotic manufacturing techniques, as well as the development and integration of an algorithm-based framework, were the emphasis of this research. The Grasshopper algorithms were verified by simulating the fabrication process using RoboDK, an offline programming tool.

The development of computational design processes and algorithmic tools for manufacturing and robotic control was one of the main objectives of this research. As a result, the automated creation of formwork geometry and its conversion into fabrication data were included in the investigation of the computational design framework. Thus, a single integrated computational workflow can accelerate both design and manufacturing processes.

- Manufacturing procedure

The manufacturing procedure for a reinforced-concrete 3D printed column is demonstrated in Figure 14. First, the column shape and fabrication data were produced and simulated using the design-to-fabrication methodology outlined in Figure 1. Following that, fabrication preparations began by developing the simulation (i.e. digital prototyping) for fabricating the column using the mechanical properties of the concrete mortar, which represent the printing filament.

The 3D prints were conducted in the facilities of the Dutch company Vertico. The ABB 6640 robotic manufacturing arm, mounted on a 6-meter track, was used for the prints. The robotic arm was capable of erecting structures up to three meters in height, and the column was realised and manufactured in the following sequence. First, the robotic arm printed the outside contours, which acted as formwork for the concrete. Second, steel bars were placed into the printed formwork in accordance with SBC 304 requirements. Third, self-consolidating concrete C40 was poured into the printed concrete formwork. This manufacturing method is further detailed throughout this paper, and the whole fabrication procedure is illustrated in Figure 14.

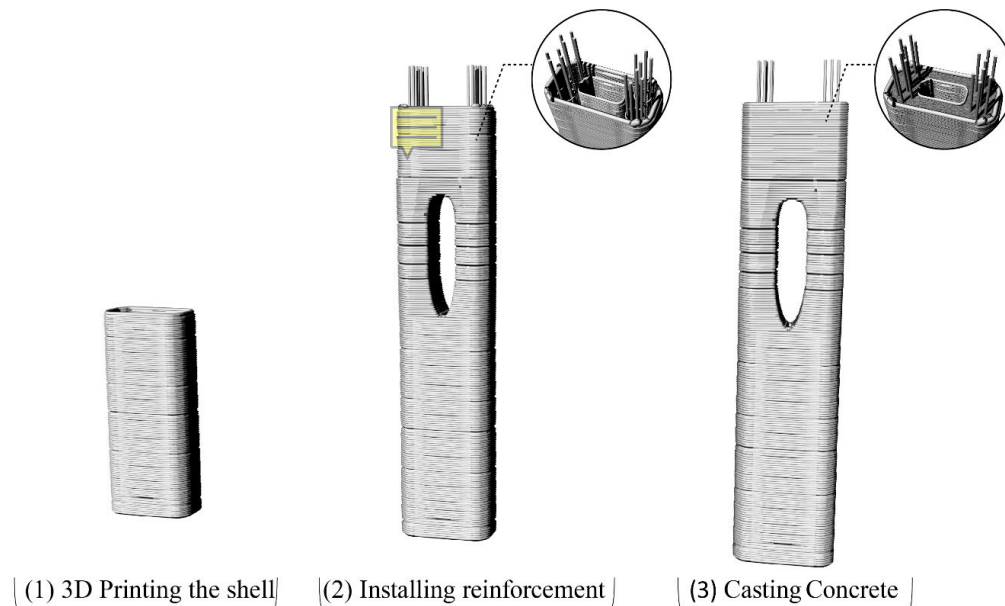


Figure 14: Fabrication procedure implemented in this research based on SBC 304: 1) 3D-printing the outer contour, 2) installing reinforcement bars and 3) casting the column with concrete

The build volume orientation has a significant impact on the feasibility and performance of AM objects, and object orientation optimisation was one of the first digital fabrication techniques used within AM. The manufacturing time, local roughness, support structure requirements and buckling were the main criteria used to assess the feasibility and realisation of the optimised structure. Framework physical validation was carried out to verify whether the computational framework was suitable for producing concrete structures in real case scenarios.

In order to avoid buckling or elastic collapse of the model, a simulated prototype was developed to assess the printing process of the model to find out the best orientation, based on the concrete filament that will be used in the 3D-printing

process. Due to the sharp overhang angle at the middle of the column, it was suggested that it would be better to flip the column upside-down to print it in one go rather than printing separate fragments and avoid unnecessary use of supporting material. The column was segmented into three manufacturing phases, as illustrated in Figure 6-18. The G code to instruct the robotic arm was generated based on the simulation in Figure 15. The next step entailed manufacturing and testing physical columns to compare the simulated model in Grasshopper with the physical models.

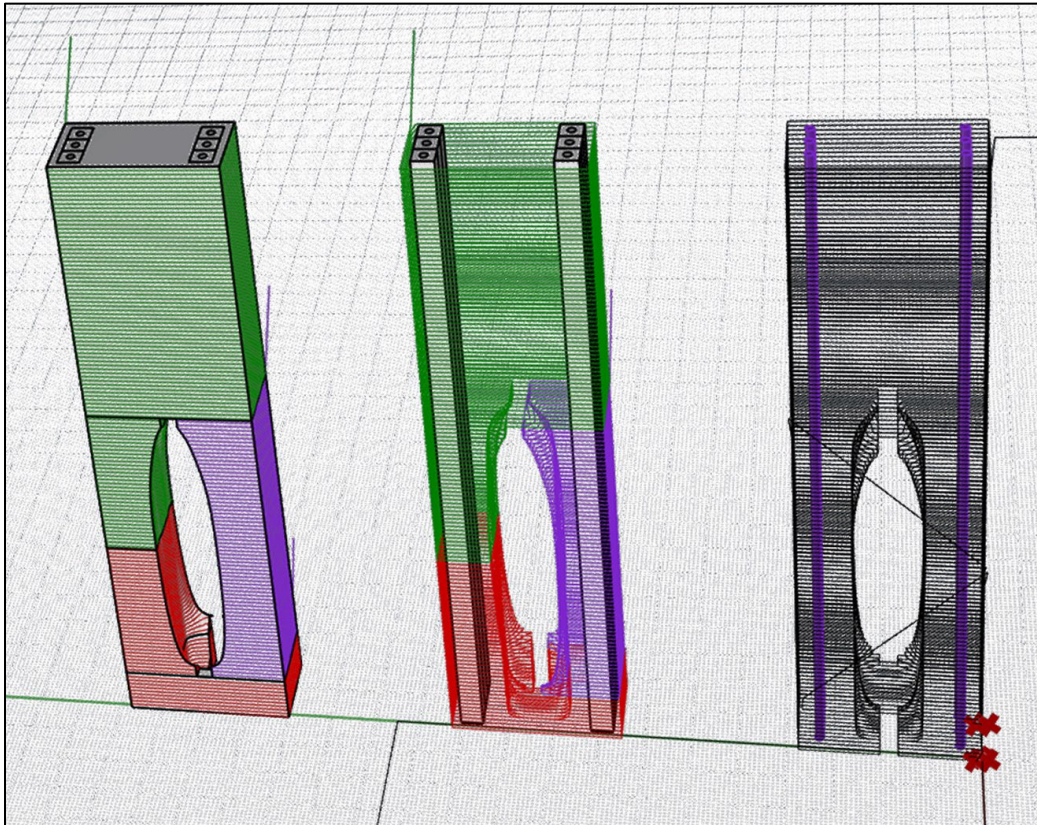


Figure 15: Slicing and segmenting the model to evaluate printability

3.2.2. Phase 2: Physical prototyping

The formal and structural potential of the construction system was proven primarily through the fabrication and validation of physical artefacts of different sizes, ranging from a small prototype to complete 3D-printed reinforced-concrete structures (Figure 16). Four robotically fabricated prototypes were created to validate the computational and physical framework fabrication processes: the first was a 1:3-scale reinforced-concrete column, the second was a 1:2-scale reinforced-concrete column, the third was a fragment of the full scale, and the fourth was the actual-scale column

(Figure 16). Based on the algorithmic TO solver (i.e. Millipede), all columns were optimised to reduce unnecessary material with the objective of minimum structural deflection.

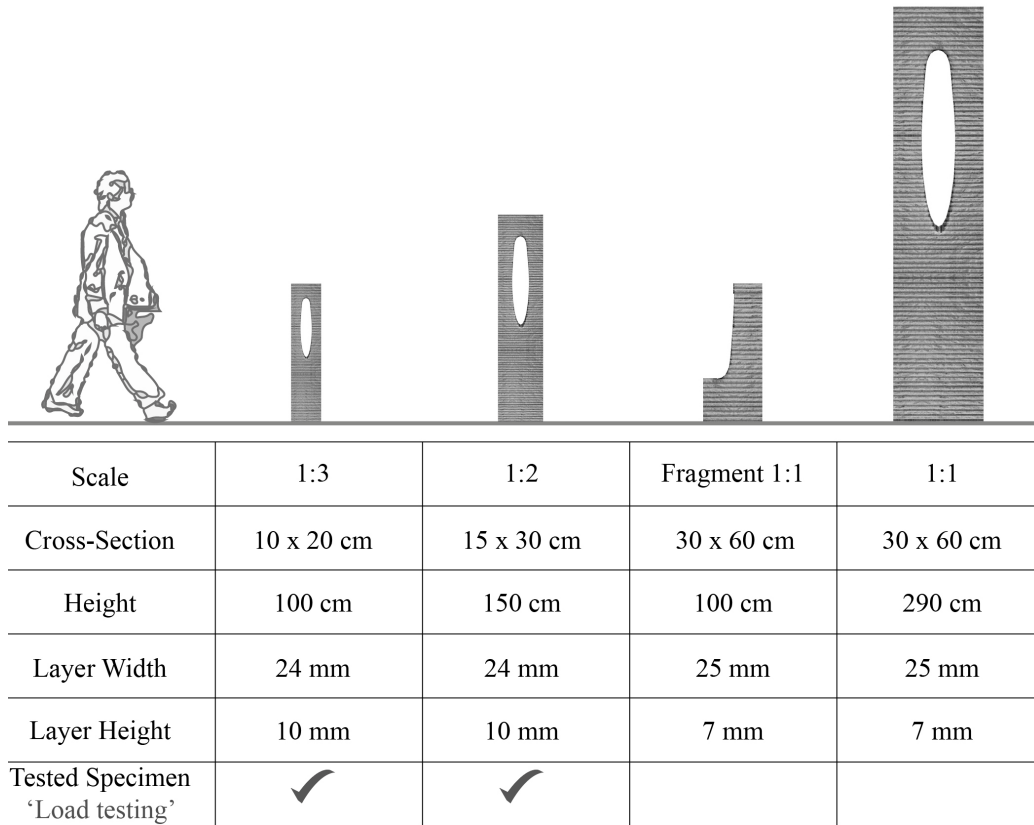


Figure 16: Comparison table to demonstrate the fabricated prototypes

The design and fabrication of the four reinforced-concrete prototypes that utilised TO techniques were tested for applicability in AM of concrete. The goal was to investigate design feasibility and identify fabrication challenges for a reinforced-concrete column using 3D-printed concrete stay-in-place formwork. The prototypes were large-scale examples of prefabricated buildings designed, to demonstrate the process's application to architecture by enabling mass customization through parametric design. The 1:1 prototype's dimensions were 0.30× 0.60× 2.90 m reinforced-concrete column. The design space was discretized into voxels, resulting in a topologically-optimised material distribution depiction.

The purpose of digital prototyping was to create a set of proper design provisions based on the fabrication constraints. The determination of design possibilities and limitations enabled the precise fabrication of the geometric complexity of the formwork in terms of the dimensions and volumetric content of concrete and required reinforcement in the concrete mixture used in the formwork. These constraints guided the final design of the four robotically fabricated prototypes in terms of rheological restrictions imposed by the concrete casting process. The robotic fabrication of the four concrete prototypes was carried out based on the fabrication strategies described in the digital prototyping phase. Furthermore, this part of the research focused on selecting concrete mixtures to meet the requirements of the entire building system under SBC 304, as well as addressing essential criteria such as concrete class, minimum reinforcement and composite structural behaviour. A significant part of the investigation conducted in this research involved examining the interrelationships of the system components and fine-tuning through iterative optimisation and physical testing.

In order to meet the SBC 304 requirements, the construction process of the column was divided into three phases, illustrated in Figure 14. They were: 1) 3D concrete printing of the formwork for the topologically optimised column, 2) insertion of 12mm steel reinforcement bars inside the concrete printed formwork and 3) casting the column with self-consolidating concrete. The following subsections will describe each of the three steps performed in the fabrication process in detail:

- Printing the column

After the column had been accurately evaluated, sliced and segmented, the configuration was then ready to be printed. The printing of the four prototypes was divided into three categories: 1) printing scale prototypes (i.e. 1:3-scale and 1:2-scale), 2) printing a fragment of the full-scale prototype and 3) printing full-scale prototypes. The printing of the scale prototypes contained two scaled columns that were one-half and one-third of the actual scale, respectively. For the 1:2-scale column, the dimensions were 0.30 m × 0.15 m × 1.50 m (width × length × height; Figure 17). For the 1:3-scale model, the dimensions were 0.20 m × 0.10 m × 1 m (width × length × height). The printing of both 1:2-scale and 1:3-scale prototypes showed agreement (i.e. geometrical and dimensions) when compared with the simulated digital prototypes, as seen in Figure 17. For both of the scale models, the use of a 10 mm layer height was suggested, in order to reduce the variation in layer-on-layer time and so provide a more consistent and smoother print quality overall (Figure 18).

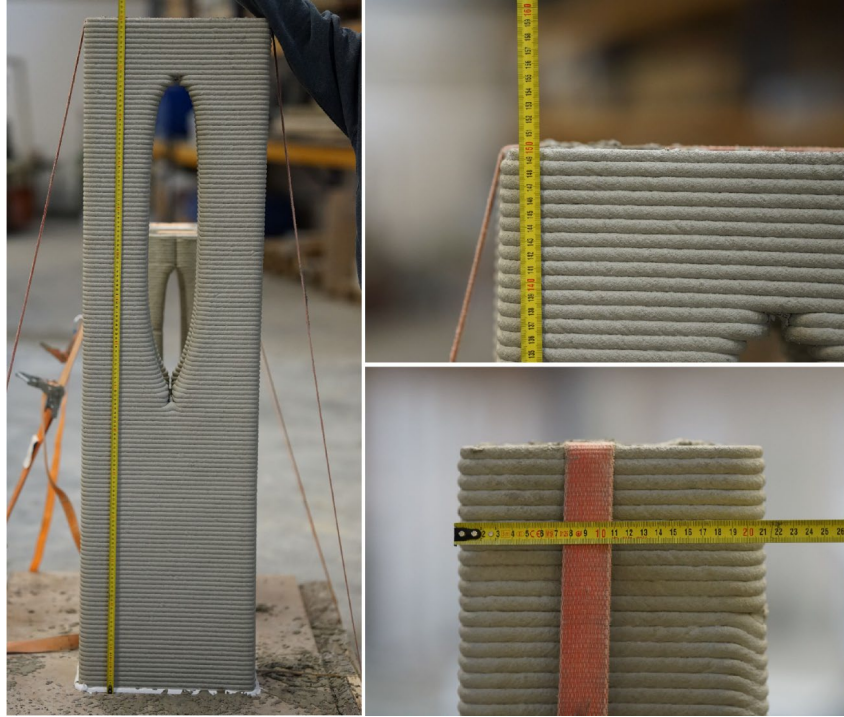


Figure 17: Documenting the dimensions of the 1:2-scale column and validating the dimensions of the printed model with the simulated model



Figure 18: Prototypes of the scaled columns (1:2-scale in the foreground and 1:3-scale in the background)

The purpose of printing a full-scale segment (Figure 19) was to ensure the feasibility of the concrete filament for realising a complex angle (e.g. overhang at the middle of the column). This model was carried out to test the printability of the sharp angle when it came to fabricating the 1:1-scale column. Accordingly, reinforcement and casting of this fragment were not required, as the performance and functionality of the structure would not be tested.



Figure 19: Printing a full-scale fragment

The full-scale prototype had dimensions of 0.60 m × 0.30 m × 2.90 m (width × length × height; Figure 6-24). It took 90 minutes to print the full-scale topologically optimised reinforced concrete column formwork without any issues. However, the time difference between printing various sections was 21 minutes. When examining the influence of the time difference from section to section, the concrete hardening and shrinkage phenomenon could be noticed on the finished print, which has been marked in blue in Figure 20.

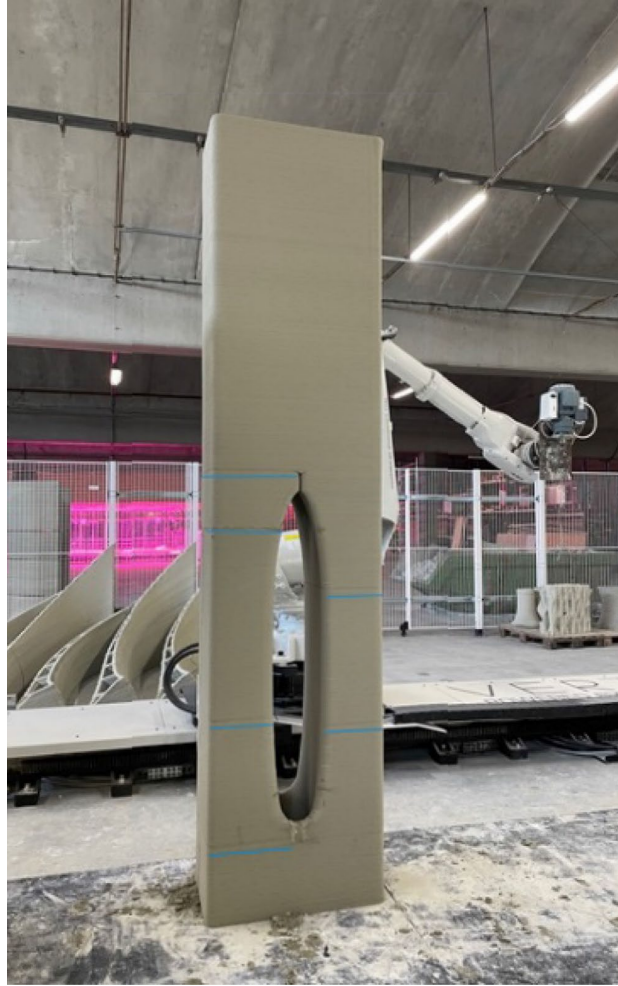


Figure 20: Full-scale prototype

Due to the start-stop technique, the longer section-on-section duration resulted in slightly higher and narrower lines because the layers on top were delayed in their placement. This was obvious because the wide layers produced a little shadow on the 'uncompressed' earlier layer that was visible due to the wide layers.

It was projected that where the section-on-section period was 21 minutes, layer adhesion would be marginally reduced, but the reduction would be significant enough for the intended utilisation in the context of this research. The transportation of the column, which was carried by straps attached to the column's centre hole, revealed the bond performance of the adhesion layers (Figure 21). The column could hold its own weight, which clarified the bond between the printed concrete layers.



Figure 21: Transporting the column using straps attached to the centre hole of the column

- **Placing reinforcement**

The 1:2- and 1:3-scale columns were reinforced with six longitudinal steel bars of 12 mm in diameter, in accordance with SBC 304 requirements for minimum reinforcement (Figure 22). Moreover, the full-scale column was reinforced with 4×4 longitudinal steel bars of 12 mm in diameter, with horizontal steel ties of 10 mm in diameter spaced at a distance of 145 mm, in accordance with SBC 304 requirements (Figure 23).

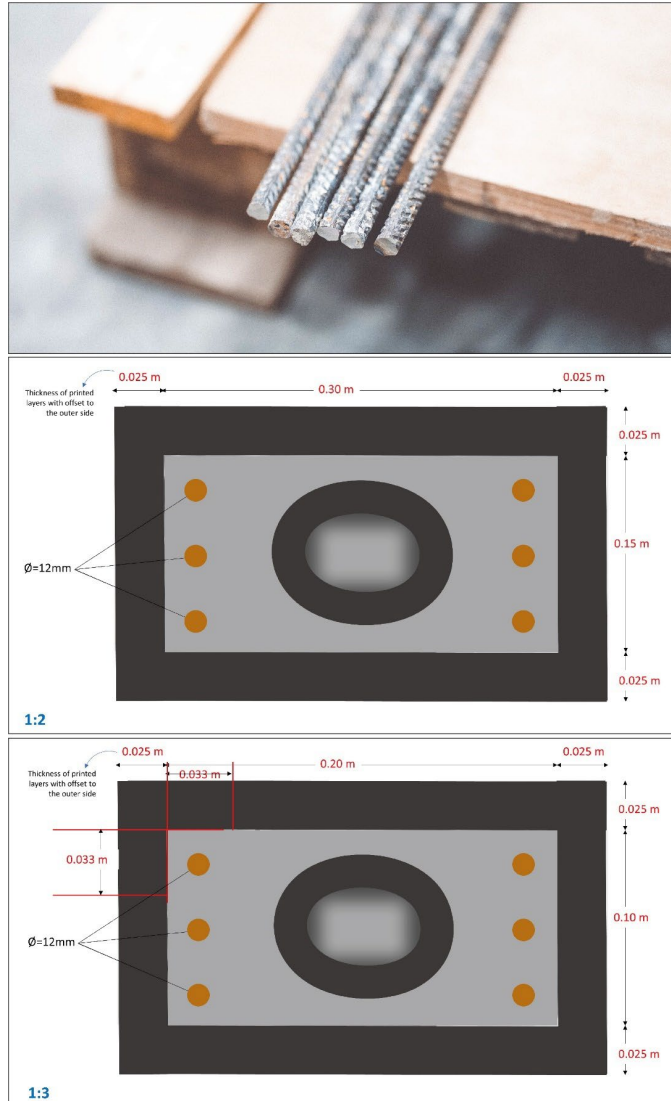


Figure 22: Top: 12 mm steel bars used to reinforce both the scaled columns, Middle: Reinforcement scheme for the 1:3-scale column, Bottom: Reinforcement scheme for the 1:2-scale column



Figure 23: Reinforcing the full-scale column with rebar 4 cages; each cage has 12 mm longitudinal bars

- **Casting the concrete**

Due to the tight space inside the 3D-printed concrete formwork, self-compacting concrete was proposed for casting the column, with a minimum strength class of C40. The main advantage of using self-compacting concrete is the workability and durability of the concrete mortar flowing inside the robotically fabricated formwork. There would be no need for a vibration device to consolidate the concrete, whereas vibration could cause unnecessary hydrostatic pressure on the 3D-printed concrete formwork, which could eventually damage the 3D printed layers of the mould. As a result, a unique mortar combination including SF2 with a minimum strength class of 40 N/mm² was produced. The mixture contained the following: quartz sand (50–75%), Portland cement (25–50%), calcium oxide (3%), calcium aluminium sulphate (1%) and crystalline silica (1%).

After determining the ingredients and ratios for the C40 self-consolidating concrete, preparation of the concrete 3D printed formwork was started for the casting. In the first steps of the casting process, the formwork was pre-wet and adhered to the support (Figure 24). As an added precaution, all prints were secured with straps to prevent the formwork from being cracked by pressure caused when the concrete was poured (Figure 25).



Figure 24: Adhering the 3D concrete printed formwork before casting with self-compacting concrete



Figure 25: Securing the prints with straps to prevent potential hydrostatic pressure between printed layers when the concrete was poured

The preparation of the mortar began as soon as the printed formwork was ready for casting (Figure 26). The mortar was made out of a two-part combination, to which 70% of the water was added initially, followed by 30% of the water coupled with an admixture to reduce shrinkage and achieve the desired workability while retaining the strength class. After the mixture had been prepared, the casting process began and was performed using the conventional manufacturing approach. Moreover, the columns were covered with plastic sheets to prevent spilling concrete from getting onto the printed surface during the process of pouring the self-compacting concrete (Figure 27).



Figure 26: Preparing and mixing the self-compacting concrete

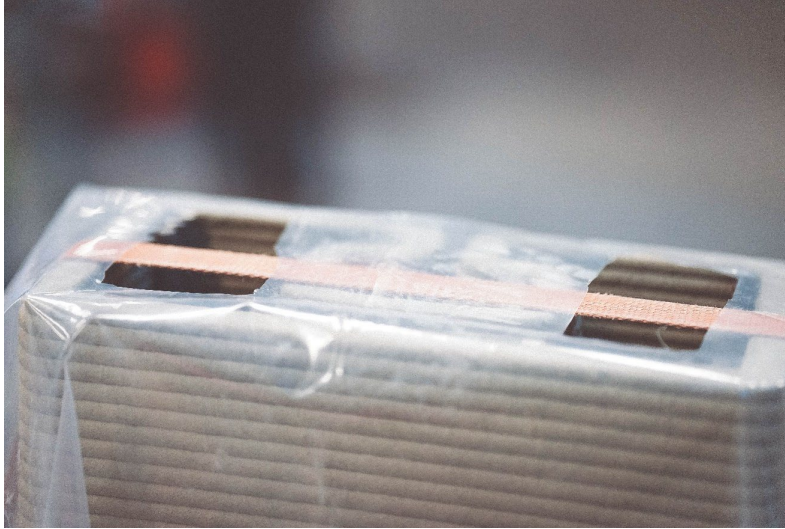


Figure 27: Covering the outer printed surface with a plastic sheet to protect the concrete from spilling while it was poured

To ensure the correct placement of the steel bars, the reinforcement was installed after the column had been cast for one-fifth of its whole length. In order to ensure that the reinforcement was properly positioned, the remainder of the column was cast until it was completely filled, and the placement of the reinforcement was checked during the casting process (Figure 28). It is worth mentioning that casting C40 self-compacting concrete inside both the 1:2- and the 1:3-scale prototypes of the columns was successfully poured inside the 3D-printed topologically optimised concrete formwork.



Figure 28: Completed reinforced concrete prototypes

Furthermore, a total of two 3D-printed concrete columns were robotically fabricated to cast the full-scale prototype column. However, due to the anticipated hydrostatic pressure during the casting process, it was essential to inspect the 3D-printed formwork before casting to prevent hydrostatic failure. It was found that the performance of the 3D-printed concrete was high in withstanding compression but weak in resisting tensile pressure. Moreover, a high tensile capacity was necessary due to the column's rectangular form to withstand the outward casting pressures. In the first attempt of 3D-printing the full-scale formwork, there were major concerns about tensile stresses due to breaking occurring at the bottom of the column during its transportation and preparation for casting, with the hydrostatic pressure greatest at the bottom (Figure 29).

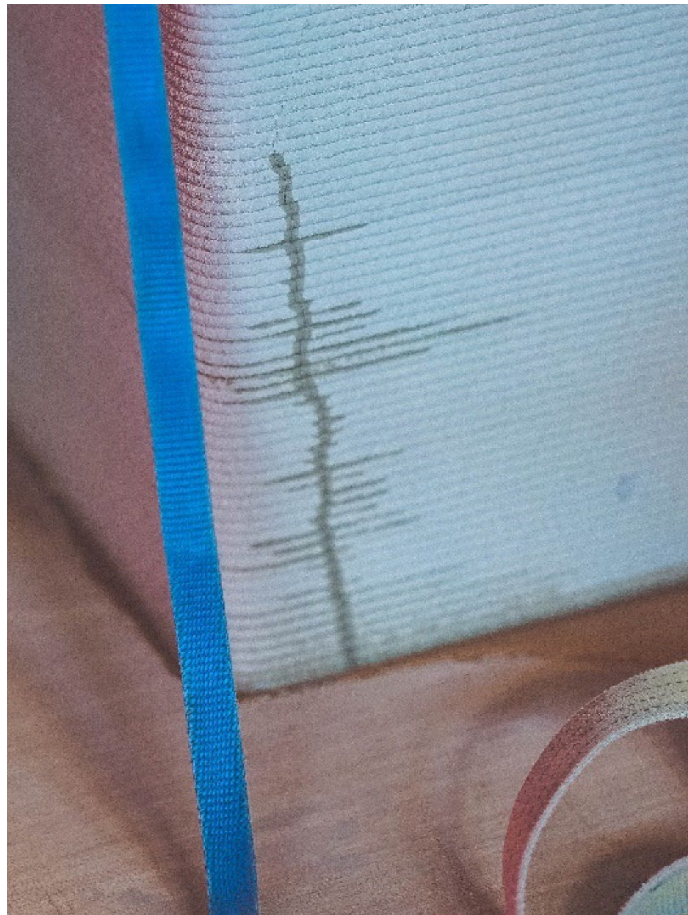


Figure 29: Cracking was visible during the first full-scale printing attempt

The second full-scale printed prototype passed the inspection phase and was ready to move into the casting phase. However, during the casting process, cracking developed after two-thirds of the column was cast with self-compacting concrete (Figure 30). The cause of the crack was most likely the consequence of the combined impact of tensile stresses caused by the shrinking of the printed geometry and the hydrostatic forces. The mechanical properties of the concrete filament and the width of the printed layers play a substantial role to withstand tensile and compression.

As the pressures advanced through the different layers, it could be seen that the layer adhesion was impressive (Figure 31), but at the point when the time difference between layers was 21 minutes, enough force had built up to break the formwork outwards (Figure 30). The outcome of the second test, following controlled demolition, is shown in Figure 32.



Figure 30: Failure of casting due to the hydrostatic pressure on the 3D printed formwork



Figure 31: A closer look at the cracks



Figure 32: Controlled demolition showing adhesion of the 3D concrete printed layers

Due to the cracks occurring on both the full-scale prototypes, the huge size of the column at the conceptual experimental level and the fact that the mechanical properties and tensile strength of the 3D-printed concrete paste were not sufficient to be integrated into the FE simulation, the full-scale column was excluded from the structural test involving applying axial load. Accordingly, the 1:2-scale and 1:3-scale printed columns were transported to the Eindhoven University of Technology to perform structural load testing.

3.3. Stage 3: Structural load testing

Along with the physical prototypes of the topologically optimised, 3D-printed reinforced-concrete column, a testing device was built to apply the axial load case into the concrete specimens. It was vital to verify the maximum deformation of the apparatus during the testing and that loads were distributed uniformly throughout the experiments, even if the system had an unbalanced settlement (Figure 33). Consequently, soft boards were used to support the specimen both below and above to provide a smooth levelling between the concrete prototypes and the load testing machine. This would also help prevent unexpected stresses because of imperfections in the surface of the concrete. The load testing of the column started with the 1:2-scale prototype. The load applied to the column was based on cyclical steps.

Due to the fact that many TO methods employ the system's compliance as an objective function, quantifying the deflections was desired at each of the system's point forces. As seen in Figure 33, the topologically optimised reinforced-concrete column was put into the testing equipment that was fitted on a load testing machine. Four LVDTs were mounted to concrete specimens in such a way that the front and rear of the specimens were firmly fastened to sturdy steel plates and rested beneath the specimen, which provided stresses. Force was applied using a displacement-controlled technique, and both forces and deflections were measured throughout the experiments. Although the column had been built for elastic behaviour, samples should be tested to failure to obtain data at both design load and beyond the optimisation's limitations.



Figure 33: The setting of the structural load test

The cyclical loading steps of the tests were implemented on the 1:2-scale reinforced-concrete column to assess its mechanical characteristics. The maximum capacity of the compression machine was 80 kN. The testing of the column took 3 hours due to the cyclical steps. The loading rate increased at 5 kN intervals for the first eight cyclical steps until 40 kN was reached. At this point, the axial load of the testing machine was left to continue until the load cell limit of 80 kN had been reached. However, the performance of the 3D printed reinforced-concrete column exceeded the prescribed loading condition, which was part of the topology optimisation objectives (Figure 7). However, this force was insufficient to fracture the 1:2-scale column to detect the actual compressive strength. Only a few cracks appeared on the 3D-printed surface, which is common for 3D-printed concrete (Figure 34). The test configuration is depicted in Figure 35. Although the column had been built for elastic behaviour, samples were tested to failure to obtain data at both design load and beyond the optimisation's limitations.





Figure 34: Small cracks appeared on the printed surface of the 1:2-scale prototype after applying a load test of 80 kN

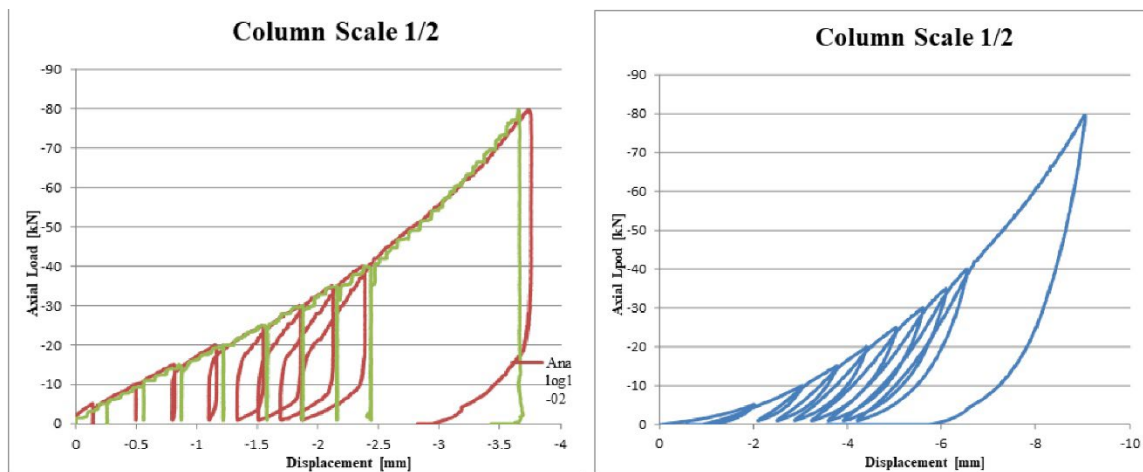


Figure 35: Displacement of the 1:2-scale prototype under axial mechanical load up to 80kN

It was suggested that the other prototype (1:3-scale) be tested to failure by using another load-testing machine with a greater loading capacity. The 1:3-scale prototype was fitted into the load testing machine (Figure 36). Four LVDTs were used to measure the displacement of the column when applying axial load. The LVDTs were installed using a similar method to that described previously for installation in the 1:2-scale prototype.

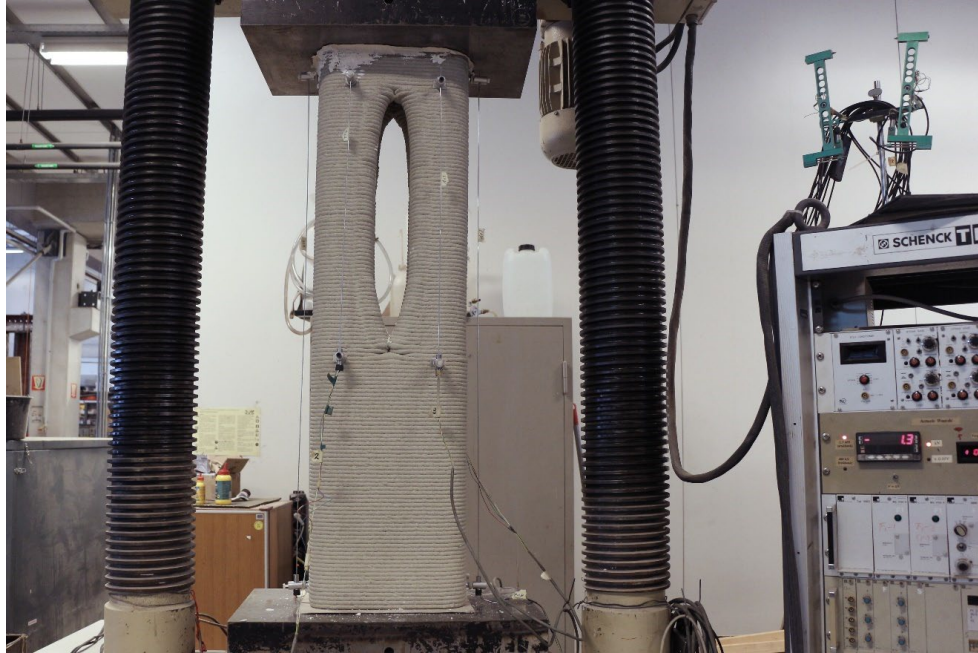


Figure 36: Fitting the 1:3-scale model into the load-testing machine

Because of the loading machine's greater capacity and the resilience of the reinforced concrete prototype, a low loading rate of 0.05 mm/min was employed to increase the axial load. Figure 37 shows the displacement curves of LVDT sensors under this loading speed. The results show that the force's initial rate was minimal, but that it increased during the test. The total time spent testing the column at a speed of 0.05 mm/min was about 2 hours. The column displacement based on the LVDTs measurements are 2.75mm and 1.50mm (Figure 37), with a jack displacement of 3.5mm (Figure 38), the maximum load to the failure point was 1475 KN. The compressive strength was calculated based on the following equation:

$$\text{Compressive Strength} = \text{Max Loading} / \text{Loading Area} \quad \text{☺}$$

$$\therefore \text{Compressive Strength} = 1475 \text{ kN} / 0.02 \text{ m}^2 = 73750 \text{ kN/m}^2 = 73.7 \text{ MPa}$$

The compressive strength of the 1:3-scale concrete column is 73.7MPa, obtained after converting the result of the previous equation from kN/m² to MPa by dividing the result by 1000.



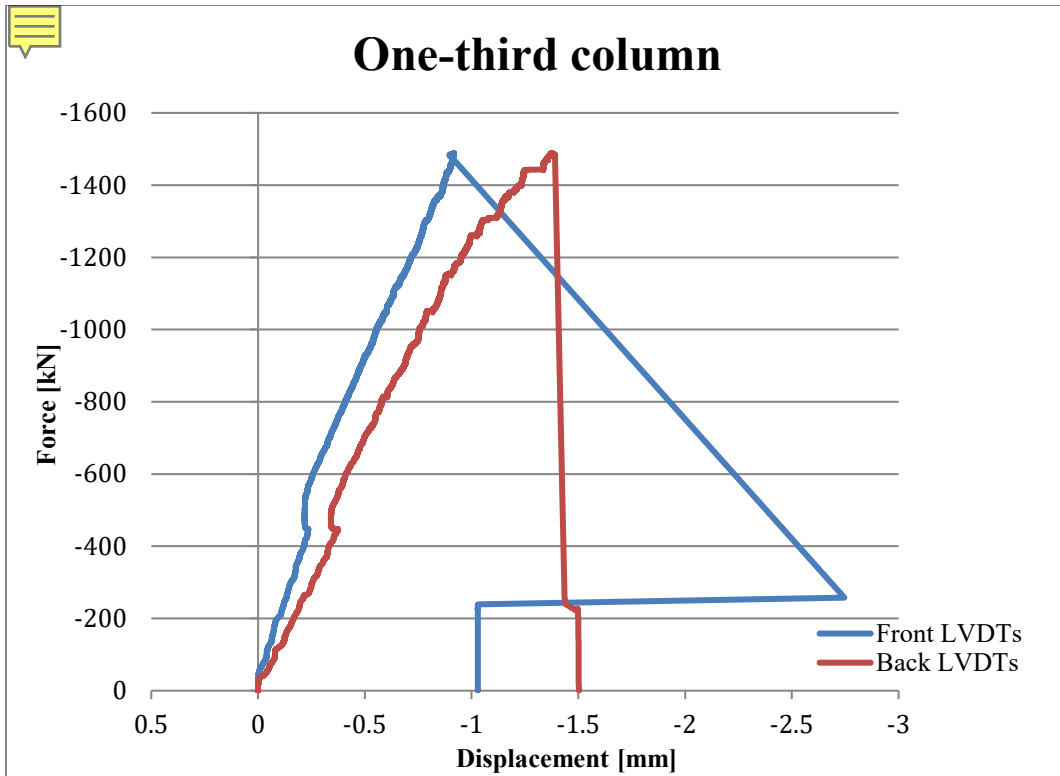


Figure 37: LVDTs measurements illustrating structural displacement

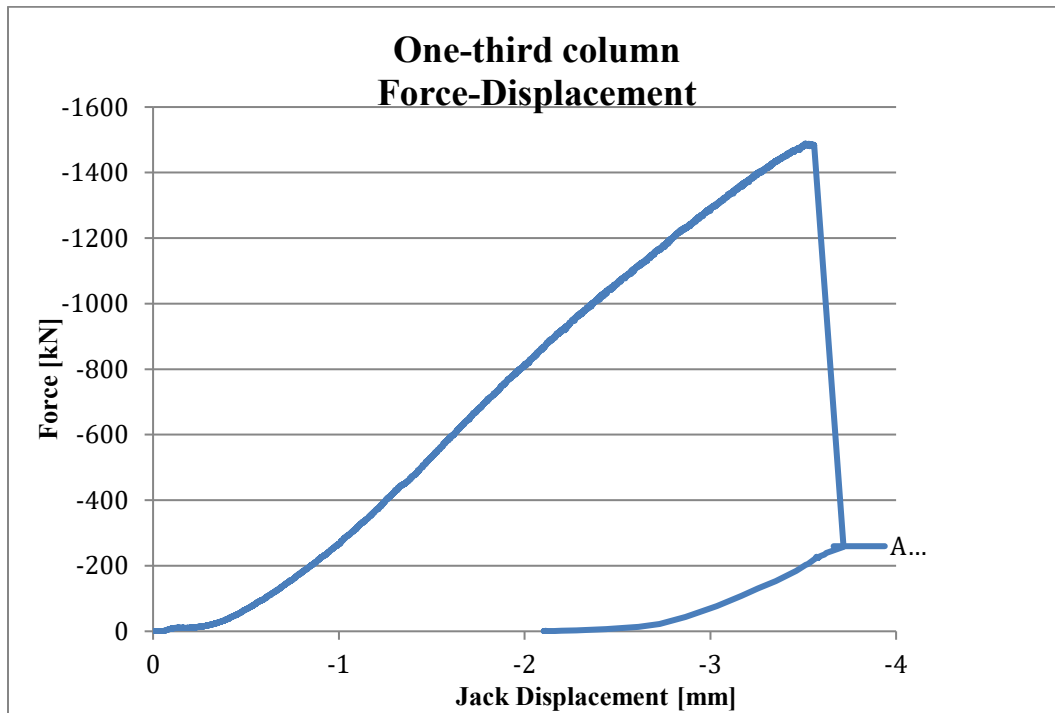


Figure 38: One can see the axial force applied on the column and jack displacement

Figure 39 demonstrates that the addition of steel bars and self-compacting C40 concrete to the column was crucial to give it the required robustness, resulting in a better post-peak response of the column. In the case of C40 concrete specimens, the damage included splitting and shear, and in the case of steel bars inside the prototype, bending of the steel occurred, as illustrated in Figure 40, after removing the prototype from the load-testing machine. For the overall specimen, cracks were found along the middle of the side and in the centre of the specimen's front and back, as illustrated in Figure 39.



Figure 39: Demonstrating the failure mode of the 1:3-scale prototype after load testing



Figure 40: After removal from the compression machine. Light grey shows the printed concrete, and dark grey shows cast concrete

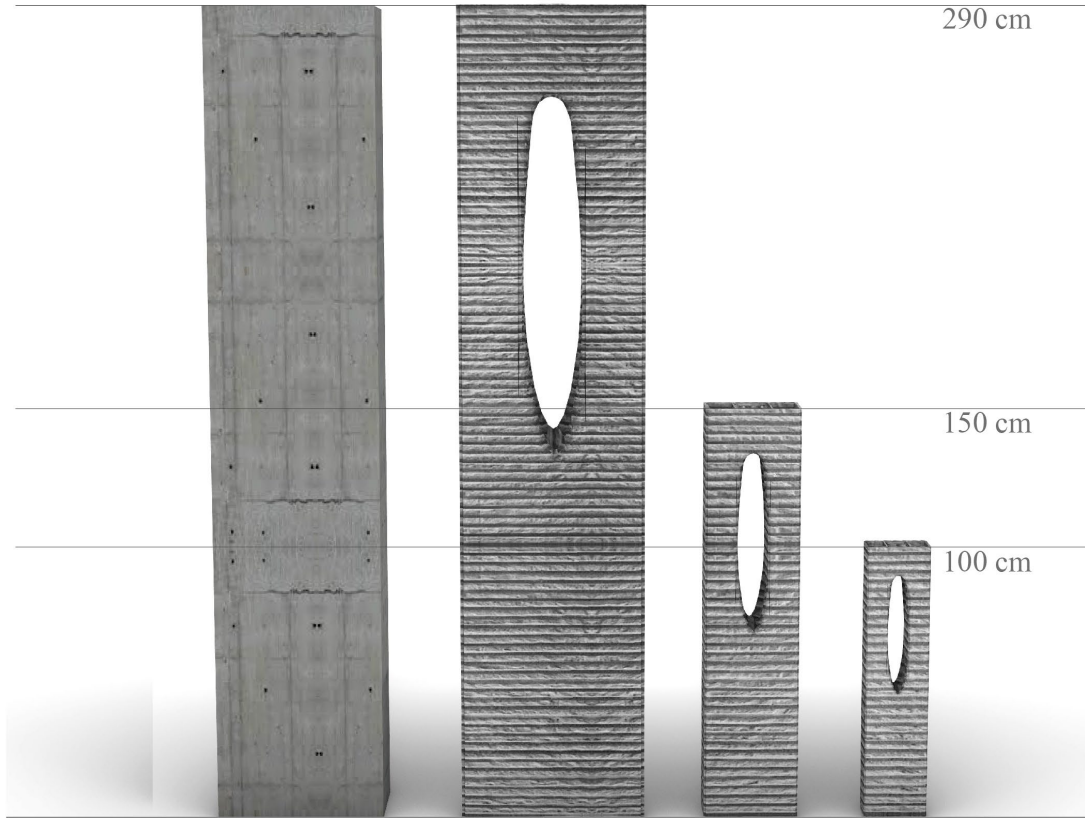
4. Findings

The main findings involved evaluating the feasibility and robustness of the proposed design-to-fabrication framework focusing on the design, TO, and robotic fabrication of four physical prototypes of a reinforced concrete column. The full size of the column was $0.30 \times 0.60 \times 2.90$ metres. The design idea and layout must be defined before building the parametric model for the reinforced concrete frame structure. It is also necessary to consider the relationships between the structural components when building the parametric model (e.g. the connections between columns, beams, and slabs). A GH script for structural component design and optimisation was required to comprehend the steps specified in the created framework. The script took advantage of GH's 3D parametric design environment, as well as Millipede and Karamba3D plugins, for structural TO and structural FEA simulation. Thus, integrating generative design, topology optimisation, and FEA into a single process was critical for completing the investigations necessary to gather component design data and decrease the evaluation time for choosing an optimal design iteration. To obtain the desired result, the required investigations for identifying the optimal iterations were sorted using the Galapagos GA solver.

The simulation results obtained throughout the optimisation process in Stage1 demonstrated that the GA solver was necessary for obtaining the most significant values from the optimisation results. The optimum results generated by the solver, in contrast to the pre-set optimisation boundaries and conditions (e.g. reinforcement), revealed the outcomes

that should be considered in the component design process. The shapes of TO results could not have been predicted or specified in advance. Furthermore, the optimisation and FEA findings for the components retrieved by the GH script and GA solver were critical for the construction of physical prototypes and the topology-optimised reinforced concrete column at an architectural scale. After defining the TO conditions, the GH script had to be modified to predefine the positions of steel reinforcement manually in the optimisation process to meet the SBC 304 standards.

The inherent digital aspect of the AM design process offers many design possibilities. Digital data connected with the design specification process includes numerical values relating to design constraints and objectives, a digital definition of spatial limits and associated boundary conditions. Therefore, it was possible to build completely algorithmic AM systems using digital algorithmic design methods, with design decisions applied using high computational rates and data bandwidths. The benefits of advanced digital algorithmic methods allow the creation of extremely complex designs using generative design methods, allowing for the use of novel design approaches and advancing the prospect of an algorithmic design framework for practical implementation. Thus, computational design opportunities allow for the early specification of high-level AM manufacturing data and its formal incorporation into the related CAD environment, providing data security for designers who plan to outsource production to independent third parties.



	Conventional	Prototype 1:1	Prototype 1:2	Prototype 1:3
Sections & Reinforcement				
Design Process	Conventional	Generative design	Generative design	Generative design
Formwork Preparation	Manual preparation "plywood"	3D printing concrete	3D printing concrete	3D printing concrete
Concrete volume	100 % (6.66992123000000006 1e-11 m³)	60 % (4.00e-11m³)	60%	60%
Height	2.90 cm	2.90 cm	150 cm	100 cm
Cross-section	0.30 x 0.60 cm	0.30 x 0.60 cm	0.15 x 0.30 cm	0.10 x 0.20 cm
Prints layer Width		25mm	24mm	24mm
Labour In-situ	Carpenter, foreman an architect and engineer	Robot operator & Foreman	Robot operator & Foreman	Robot operator & Foreman
Physical Load test				1475 kN Failure load
Compressive Strength				73.5MPa

Figure 41: Comparison between a conventional column and developed columns

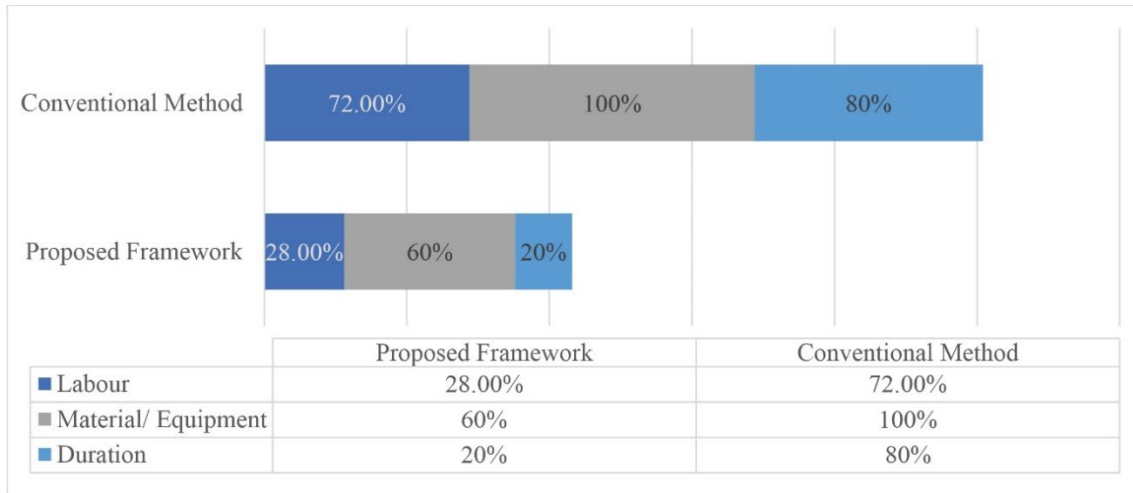


Figure 42: Comparison between conventional construction of a column with the digitalised method

5. Discussion

As a solution to the housing construction problems in the KSA, the design-to-fabrication algorithmic framework proposed in this research provides numerous potential benefits for architecture, structural engineering, and relevant fields such as material science. The study's findings provided evidence for topologically optimised structures' design, assessment, and manufacturing potential. A parametric GH script was also created to manage the frame structure of a typical Saudi villa.

The purpose of the design-to-fabrication framework developed in this research was for analysing, optimising, and testing concrete structural components throughout the conceptualization, prototyping, and testing stages. Designers should be able to use the script to design and optimise various structural components (e.g. columns, beams, and slabs), ascertain their viability, and prepare structural components for robotic manufacture. The control parameters for the parametric villa can be incorporated into a GA solver process to perform an environmental or acoustic study, for future case studies, based on the villa's proposed location.

The created GH script was essential for manufacturing the experimental column, including slicing the column, determining sharp angles (e.g. overhang), suggesting fabrication strategies, and generating robotic G-code instructions. The calibration of the mechanical characteristics of the printing filament and the created GH script should be considered before the manufacturing process (e.g. digital prototyping phase). Therefore, the TO and 3D printing

simulation of a typical column showed the proposed framework's effectiveness to address concerns like labour shortages and construction duration in practical construction in the KSA. A comparison of the material consumption in conventional and optimised columns found that the material volume of the optimised column was lowered by 40%. Furthermore, the use of unnecessary plywood in the construction of the concrete formwork was eliminated. Thus, the material could be further reduced based on the physical test (Figure 41). Furthermore, robotic technology in conjunction with AM could reduce the amount of labour required on a building site by 28% (Figure 42).

Moreover, the time required to print the column was decreased by 80% since the column was printed in a single process, thereby minimising construction waste and eliminating the need for labour to construct the plywood formwork. The developed framework, based on algorithmic data structure, can mitigate the design process by employing generative design and parametrically customising the house. Compared to the usual building approach, the framework can enhance the efficiency of housing construction, as shown in Figure 41. This conclusion is based on the reduction of required labour, material volume, and construction duration.

The topologically optimised reinforced 3D printed concrete column was developed with digital and physical prototypes to validate the feasibility and functionality of the proposed design-to-fabrication framework. The experiments were conducted to assess the result of computational design and its compatibility with the robotic control process that would generate intricate reinforced concrete structure elements algorithmically and transform them to manufacturing robotic fabrication instructions (i.e. G-code). Computational workflow included simulation of fabrication processes was embedded in the GH script. RoboDK was used to mimic the 3D-printing process and generate robotic instructions. Furthermore, four prototypes were fabricated to examine design feasibility and constraints using concrete 3D-printed stay-in-place formwork. The prototypes include a small prototype to check water tightness and entire 3D-printed reinforced concrete structures, which were implemented to demonstrate the construction system's efficiency and structural capabilities. Thus, the layer adhesion of concrete filament illustrated its effectiveness as the column can hold its weight. The bonding between the concrete printed layers and self-consolidating concrete revealed excellent interlocking mechanical properties, as illustrated in Figure 40, which can increase the structural performance of the topology optimised column. In addition, the implementation and validation

procedures described in this paper demonstrate that the proposed framework and the algorithmic GH script can be used to efficiently design, optimise and fabricate reinforced-concrete building components.

Furthermore, to avoid hydrostatic failure when casting the 3D-printed topologically optimised formwork, it was vital to inspect the printed formwork before casting. Although a crack developed during the pouring of self-compacting concrete inside the full-scale chambers, the speed rate of pouring the concrete, layer width, and mechanical properties of the concrete filament play crucial roles to withstand hydrostatic pressure. Furthermore, it is essential to investigate the speed rate of pouring concrete, and the orientation of the printed structure (e.g. print and cast structure horizontally), which may reduce the hydrostatic pressure.

The proposed approach could handle practical construction difficulties such as labour shortages and construction duration in the KSA. The created framework, which is built on an algorithmic data structure, can help to speed up the design process by incorporating generative design and parametric customisation. In comparison to conventional construction methods, the framework will increase the efficiency of dwelling construction, as illustrated in Figure 41. Moreover, 3D-printing of structural building components using robotic-based printers will not only improve construction production efficiency but will also address KSA citizens' customisation problems, which centralised precast manufacturing has failed to address. However, various obstacles need to be overcome to introduce robotic printing into the construction industry efficiently. The most evident issue in this research was running robots for in-situ fabrication due to various factors, including the extreme climate in the KSA due to the high temperatures and dust. It would be difficult to handle the printing of housing components during the summer without operating the fabrication process in a controlled environment. However, this issue can be tackled using a transportable robotic arm based in a shipping container (Figure 43). Thus, the mechanical properties of printing materials have a major impact on the complexity of architectural designs. Overcoming these challenges can pave the way for a revolutionary building method that can be adopted into the present SBC 304, which was the main focus of this research.

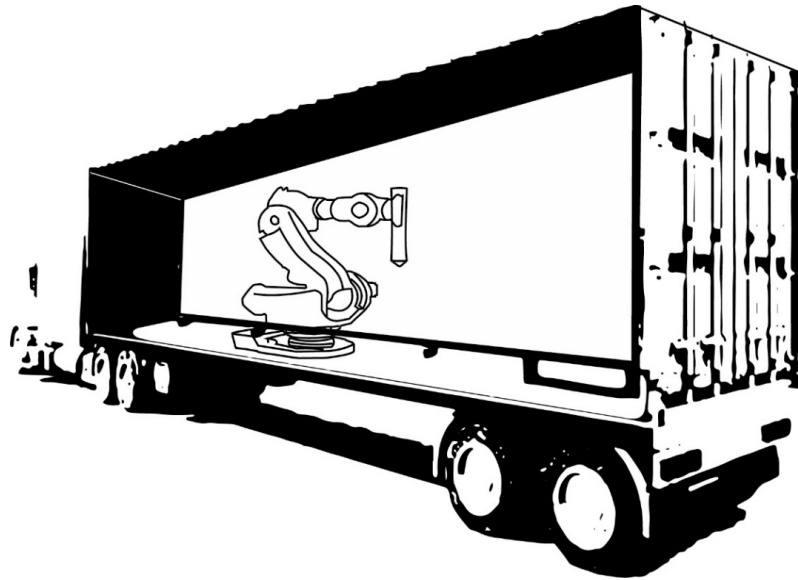


Figure 43: Transportable factory based in a shipping container

6. Conclusion

The standard TO techniques that are compatible with AM was evaluated in order to highlight the value of TO in leveraging material savings when used in conjunction with AM technology. The researchers then examined the simulation and voxelisation of the TO outputs using FEA methods. Using a generative design technique, the study examined the possible benefits of TO in load-bearing system development. Also, the research established the design-to-fabrication framework in Grasshopper, the framework examined the compatibility of AM and TO in terms of design and manufacturing as well as the suitability to be implemented under SBC304.

As a result, by abstracting the building down to its fundamental structural components, the reinforced concrete frame structure of a typical house may be optimised and readied for 3D printing (columns, beams, and slabs). The TO performed on the column demonstrated that the specifically developed approach was capable of adapting to the imposed axial loads while taking into account the material restrictions. As a result, this technology increased structural stiffness while reducing material consumption.

The developed framework contributes to the design, optimisation, and fabrication of structural components with regard to SBC304. Therefore, FE analysis was performed to determine the structural stability and verify the structure. To confirm the proposed approach to the present Saudi Code, steel bars were employed to strengthen the core sections.

This was accomplished during the detail design phase by updating the GH script to incorporate real material attributes (i.e., reinforcement allocation) from the fabrication process. The optimisation result (i.e. TO column) indicated that it may be used to construct a robotic toolpath through slicing algorithms coupled to RoboDK to generate the G-code.

The created framework's feasibility and functionality were examined by designing and fabricating a proposed 0.30 m × 0.60 m × 2.90 m (height × width × length) topology-optimised reinforced concrete column and constructing actual prototypes of various sizes. The validation procedure began with the testing of the framework on an official drawing for a typical Saudi villa, followed by GH development of the villa's parametric concrete structure. A reinforced concrete column was then considered to assess the applicability of the Millipede TO method in GH by developing a parametric GH script. The GH script integrated form generation for both the parametric frame structure and structural TO, using FEA and heuristic search techniques with the Galapagos genetic algorithm (GA) solver in a GH parametric design environment, and slicing the optimisation results to generate G-code for the robotic instructions using the off-line RoboDK programming tool. The TO process required a special procedure, which was characterised by a set of optimisation boundaries and constraints essential to the design input data for the TO solver. The developed script was then used to design, assess, and extract the design data for the GH components of the topology-optimised concrete column, employing the extracted loading conditions from the FEA model built according to official drawings obtained from the KSA's Ministry of Housing.

Subsequently, the study concentrated on the design-to-fabrication process for the topology-optimised reinforced concrete column to construct concrete prototypes. Two scaled prototypes were built and tested found that the column's shape and the tensile strength of the concrete filament used to fabricate the formwork both contributed significantly to the printed formwork's ability to withstand axial load. Additionally, the one-to-one scale column experiment demonstrated significant results regarding sustaining hydrostatic pressure during the casting process, which pave the way for future research. The developed prototypes were digitally modelled, robotically manufactured, and assessed using GH scripts. It was necessary to reinforce the column with a minimum of 12-mm steel bars to meet the SBC 304 standards [27] while fabricating the prototypes. Finally, fabrication techniques for the model were developed, which involved printing the outside contours, reinforcing them with steel, and casting them using C40 self-consolidating concrete.

In summary, this research aimed to expand AM of concrete building components horizons and contribute significantly to knowledge of the AM of concrete in housing construction. Additionally, the research identified methodologies and procedures for the design and TO of reinforced concrete structures, as well as their potential for creating bespoke reinforced concrete building components. Moreover, the research developed a design-to-fabrication framework and a GH script to assist designers in generating, investigating and evaluating the results of topologically optimised building components and smoothly preparing the components for AM.

To enhance the reliability, convenience, and accuracy of the created framework and GH script, as well as the precision of the simulation results obtained, future research is essential. Further study is required to integrate other parameters (e.g. hydrostatic pressure) into the design-to-fabrication framework. Thus, this research can be used as a basis for future research in the fields of architecture and structural engineering, both academically and practically.

ACKNOWLEDGMENTS

This is just an example. This section is optional.

REFERENCES

- [1] M. Valente, A. Sibai, M. Sambucci, Extrusion-based additive manufacturing of concrete products: Revolutionizing and remodelling the construction industry, *J. Compos. Sci.* 3 (2019). <https://doi.org/10.3390/jcs3030088>.
- [2] Statista.com, Gross domestic product of the construction sector in Saudi Arabia from 2011 to 2020, (2022). <https://www.statista.com/statistics/626547/saudi-arabia-gdp-construction-sector/>.
- [3] A. Shash, E. Al-Mulla, Major components of "typical villa" in Saudi Arabia for price/cost index development, *6th Saudi Eng. Conf.* 1 (2002) 47–62.
- [4] W.S. Alaloul, M.S. Liew, N.A.W.A. Zawawi, B.S. Mohammed, Industry Revolution IR 4.0: Future Opportunities and Challenges in Construction Industry, *MATEC Web Conf.* 203 (2018) 1–7. <https://doi.org/10.1051/mateconf/201820302010>.
- [5] S.H. Khajavi, M. Tetik, A. Mohite, A. Peltokorpi, M. Li, Y. Weng, J. Holmström, Additive manufacturing in the construction industry: The comparative competitiveness of 3d concrete printing, *Appl. Sci.* 11 (2021).

- <https://doi.org/10.3390/app11093865>.
- [6] Theodore Karasik, Saudi Housing Requirements for a Strong and Secure Future, *Int. Policy Dig.* (2017). <https://intpolicydigest.org/2017/06/09/saudi-housing-requirements-strong-secure-future/>.
- [7] A. Alqahtany, A. Bin Mohanna, Housing challenges in Saudi Arabia : the shortage of suitable housing units for various socioeconomic segments of Saudi society, *22* (2019) 162–178. <https://doi.org/10.1108/HCS-01-2019-0002>.
- [8] H. Alhubashi, HOUSING SECTOR IN SAUDI ARABIA: PREFERENCES AND ASPIRATIONS OF SAUDI CITIZENS IN THE MAIN REGIONS, Universidad Politécnica de Cataluña, 2018.
- [9] V. Mechtcherine, V.N. Nerella, F. Will, M. Näther, J. Otto, M. Krause, Large-scale digital concrete construction – CONPrint3D concept for on-site, monolithic 3D-printing, *Autom. Constr.* *107* (2019) 102933. <https://doi.org/10.1016/j.autcon.2019.102933>.
- [10] R.A. Buswell, W.R. Leal de Silva, S.Z. Jones, J. Dirrenberger, 3D printing using concrete extrusion: A roadmap for research, *Cem. Concr. Res.* *112* (2018) 37–49. <https://doi.org/10.1016/j.cemconres.2018.05.006>.
- [11] R. Comminal, W.R. Leal da Silva, T.J. Andersen, H. Stang, J. Spangenberg, Modelling of 3D concrete printing based on computational fluid dynamics, *Cem. Concr. Res.* *138* (2020) 106256. <https://doi.org/10.1016/j.cemconres.2020.106256>.
- [12] M. Alabbasi, H.-M. Chen, A. Agkathidis, Assessing the effectivity of additive manufacturing, in: 9th ASCAAD Conference Proceedings (Ed.), *Archit. Age Disruptive Technol. Transform. Challenges*, Cairo, 2021: pp. 214–226. <https://doi.org/978-1-907349-20-1>.
- [13] I. Hager, A. Golonka, R. Putanowicz, 3D Printing of Buildings and Building Components as the Future of Sustainable Construction?, *Procedia Eng.* *151* (2016) 292–299. <https://doi.org/10.1016/j.proeng.2016.07.357>.
- [14] O. Kontovourkis, P. Konatzii, Design-static analysis and environmental assessment investigation based on a kinetic formwork-driven by digital fabrication principles, *Odysseas Kontovourkis (Ed.), Sustain. Comput. Work. [6th ECAADe Reg. Int. Work. Proceedings]*, Dep. Archit. Univ. Cyprus. (2018) 131–140.
- [15] R.A. Buswell, W.R.L. da Silva, F.P. Bos, H.R. Schipper, D. Lowke, N. Hack, H. Kloft, V. Mechtcherine, T. Wangler, N. Roussel, A process classification framework for defining and describing Digital Fabrication with

- Concrete, *Cem. Concr. Res.* 134 (2020). <https://doi.org/10.1016/j.cemconres.2020.106068>.
- [16] A. Anton, L. Reiter, T. Wangler, V. Frangez, R.J. Flatt, B. Dillenburger, A 3D concrete printing prefabrication platform for bespoke columns, *Autom. Constr.* 122 (2021) 103467. <https://doi.org/10.1016/j.autcon.2020.103467>.
- [17] M. Leary, *Design for additive manufacturing*, 2020.
- [18] O. Kontovourkis, G. Tryfonos, C. Georgiou, Robotic additive manufacturing (RAM) with clay using topology optimisation principles for toolpath planning: the example of a building element, *Archit. Sci. Rev.* 63 (2020) 105–118. <https://doi.org/10.1080/00038628.2019.1620170>.
- [19] K. Januszkiewicz, M. Banachowicz, Nonlinear Shaping Architecture Designed with Using Evolutionary Structural Optimisation Tools, *IOP Conf. Ser. Mater. Sci. Eng.* 245 (2017). <https://doi.org/10.1088/1757-899X/245/8/082042>.
- [20] M. Donofrio, Topology Optimisation and Advanced Manufacturing as a Means for the Design of Sustainable Building Components, *Procedia Eng.* 145 (2016) 638–645. <https://doi.org/10.1016/j.proeng.2016.04.054>.
- [21] A. Bacciaglia, A. Ceruti, A. Liverani, A systematic review of voxelization method in additive manufacturing, *Mech. Ind.* 20 (2019) 630. <https://doi.org/10.1051/meca/2019058>.
- [22] A.O. Aremu, J.P.J. Brennan-Craddock, A. Panesar, I.A. Ashcroft, R.J.M. Hague, R.D. Wildman, C. Tuck, A voxel-based method of constructing and skinning conformal and functionally graded lattice structures suitable for additive manufacturing, *Addit. Manuf.* 13 (2017) 1–13. <https://doi.org/10.1016/j.addma.2016.10.006>.
- [23] M. Abdi, Evolutionary topology optimisation of continuum structures using X-FEM and isovalues of structural performance, Univ. Nottingham. PhD thesis (2015).
- [24] F. Laverne, N. Anwer, M.L.E. Coq, I.U.T. St, P. Tech, L. Cpi, E.N.S. Cachan, C. Cedex, DFAM in the design process: A proposal of classification to foster early design stages, *Confere 2014.* (2014) 1–12.
- [25] SBCNC, Saudi building code national committee, 2018. <https://doi.org/10.1017/CBO9781107415324.004>.
- [26] A. Tedeschi, *Algorithms Aided Design*, Le Penseur, 2014.
- [27] SBC Committee 304, *Structural - Concrete structures*, (2007) 274.

